THE DESIGN AND PERFORMANCE OF THE NEW ECMWF OPERATIONAL MODEL

A.J. SIMMONS AND M. JARRAUD

European Centre for Medium Range Weather Forecasts

1. INTRODUCTION

A new atmospheric model was introduced into operational forecasting at ECMWF on 21 April 1983. The principal differences between this model and the Centre's first operational model are in the adiabatic formulation, which in the new model includes use of a spectral representation in the horizontal, a more general vertical coordinate, and a modified, more-efficient, time-stepping scheme. In addition, new programming techniques and standards have been adopted to facilitate both the model's use as a research tool and its adaptation to make full use of the features of the CRAY X-MP computer recently acquired by ECMWF. A number of revisions have also been made in detailed aspects of the formulation of the parameterization schemes. The operational change to this new model was accompanied by a second important change, namely the use of a higher 'envelope' orography in the lower boundary conditions of the model.

Much of the evidence on which the decision to make these changes was based has already been presented in contributions to ECMWF's publication series. Girard and Jarraud (1982) described an extensive experiment in which the then-operational 1.875° grid-point model forecasts were compared once a week for a year with forecasts made using a spectral model (Baede et al., 1979) with triangular truncation at total wavenumber 63 (T63). The two models used identical parameterization schemes and required similar amounts of computing resources. The results of these and subsequent comparisons are summarized in the preceding contribution to these proceedings, and show that although the two models often gave very similar forecasts, there were some clear differences in favour of the spectral method. The new vertical formulation is that presented by Simmons and Strüfing (1981), who showed some small benefit to arise from replacement of the classical sigma coordinate by a 'hybrid'

coordinate which is terrain-following at low levels but which tends continuously to a pressure coordinate at upper levels. The diagnostic study and preliminary forecast experiments supporting use of the envelope orography have been reported by Wallace et al.(1983).

In this paper we outline a number of features of the formulation of the new forecast model, including results from some of the short series of tests carried out during its development. Results are also presented from two final pre-operational trials. The first of these comprised weekly forecasts from the winter of 1982/83 using initial data prepared operationally using the grid-point model in the data assimilation and the then operational grid-square mean orography. The second comprised a sequence of 19 daily forecasts starting from 2 April 1983 in which the new forecast model and envelope orography were used in a strict repetition of the operational forecasting procedure, including the data assimilation. Some aspects of the performance of the new model and orography in full operational use will also be discussed.

2. IMPLEMENTATION OF THE SPECTRAL TECHNIQUE

The mathematical formulation of the spectral transform technique adopted for the model largely follows the approach of the first multi-level spectral models of Bourke (1974) and Hoskins and Simmons (1975), and in particular that of the original ECMWF spectral model (Baede et al., 1979). Basic details are as given in our general lecture on the spectral technique presented in these proceedings, and little elaboration is needed here. For the temperature and humidity equations, explicit grid-point tendencies are computed prior to the transformation to spectral space, using grid-point values of horizontal gradients of T and q. With this formulation, and a data-scanning structure which gives grid-point values of the prognostic variables at the previous as

well as the present timestep, a general programme organization similar to that of the model's operational predecessor could be adopted. Thus tendencies due to all adiabatic and parameterized processes are calculated in a single scan of grid-point space, using an explicit timestep to calculate the new time-level values required for the computation of precipitation and latent-heat release. The semi-implicit time-stepping scheme (see section 4) is implemented as a subsequent correcting factor, with computations performed in grid-point, Fourier or spectral space as appropriate. This yields a relatively straightforward structure of the code performing the central dynamical and physical calculations, and facilitates the provision of diagnostics.

Apart from this aspect of the implementation of the spectral technique, the other points worthy of note relate to the efficiency and flexibility of the calculation. Grid-point and Fourier space computations are performed alternatively for Northern and Southern Hemispheric latitudes, enabling use of equatorially symmetric and anti-symmetric Fourier components in a more efficient calculation of Legendre transforms. The efficiency of these transforms has also been improved by ordering their computation in a way different from that used in the Centre's original spectral model. The horizontal truncation of the spectral expansions is flexible, allowing use of either one of the common truncations or a more extreme form which may be useful for specific investigations. The truncation may also vary in the vertical. Some provision has also been made to use less points around latitude circles close to the poles than are formally required for alias-free calculation of quadratic terms, although this has yet to be tested. The model has in addition been formulated to allow alternative data-scanning structures to be used. This enables a choice to be made between the central-memory requirement of the model and its requirement for input/output

involving secondary storage devices, and gives a potential for high resolution experimentation and efficient use of available computing resources.

The truncation adopted operationally is triangular at wavenumber 63, as used in the earlier comparison with the 1.875° grid-point model. The computations in physical space are performed on a grid comprising 192 points distributed regularly around each of 96 'Gaussian' latitudes. A complete specification of the model, with more extensive references, will be found in the appropriate documentation manual available from ECMWF.

3. VERTICAL REPRESENTATION

The vertical finite-difference formulation of the new model is that described by Simmons and Strüfing (1981). It differs little from that of the Centre's earlier models, but has been designed to allow a more general vertical coordinate to be used. The new model can use any coordinate for which model layers are defined by interfacial pressures of the form:

$$p_{k+1/2} = A_{k+1/2} + B_{k+1/2}\, p_s$$

for k = 0, 1, 2, ...N. Here p_s is the surface pressure, N is the number of model layers, and the $A_{k+1/2}$ and $B_{k+1/2}$ are constants which must satisfy:

$$A_{1/2} = B_{1/2} = 0; \quad A_{N+1/2} = 0, \; B_{N+1/2} = 1$$

The classical sigma coordinate adopted for the Centre's earlier models is a special case for which $A_{k+1/2} = 0$ for all k.

Table 1 Parameters determining the vertical resolution of the new operational model

k	$A_{k+1/2}$ (Pa)	$B_{k+1/2}$
0	0	0
1	5000	0
2	9891	0.00172
3	14166	0.01320
4	17346	0.04222
5	19121	0.09376
6	19371	0.16957
7	18164	0.26802
8	15742	0.38427
9	12488	0.51083
10	8882	0.63827
11	5438	0.75638
12	2626	0.85561
13	783	0.92875
14	0	0.97299
15	0	0.99228
16	0	1.00000

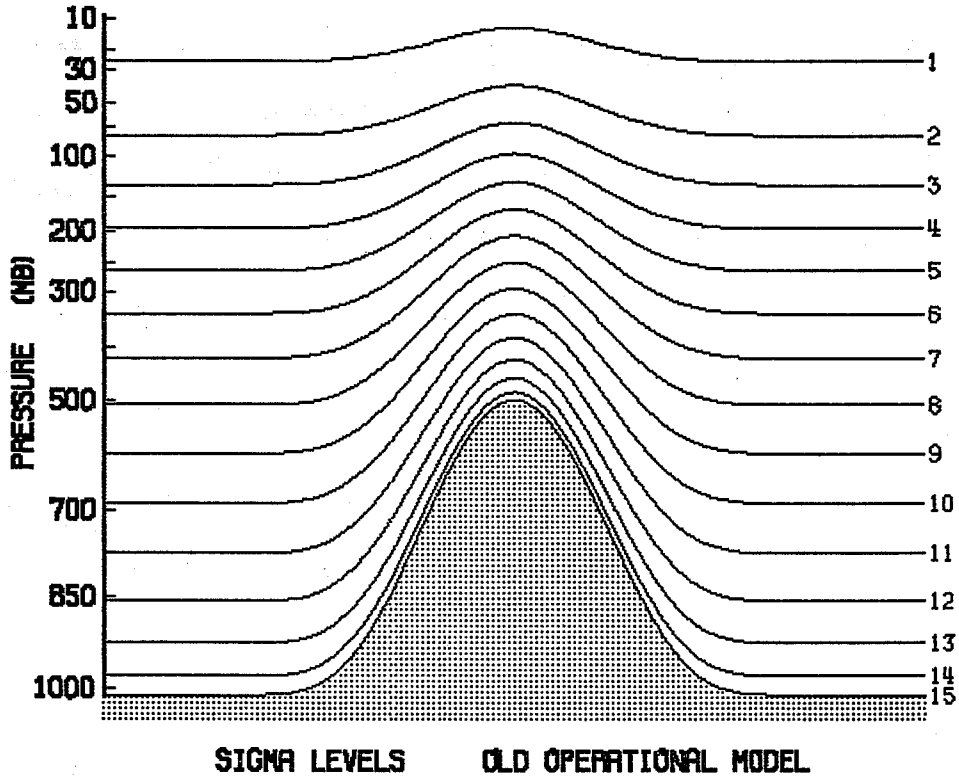

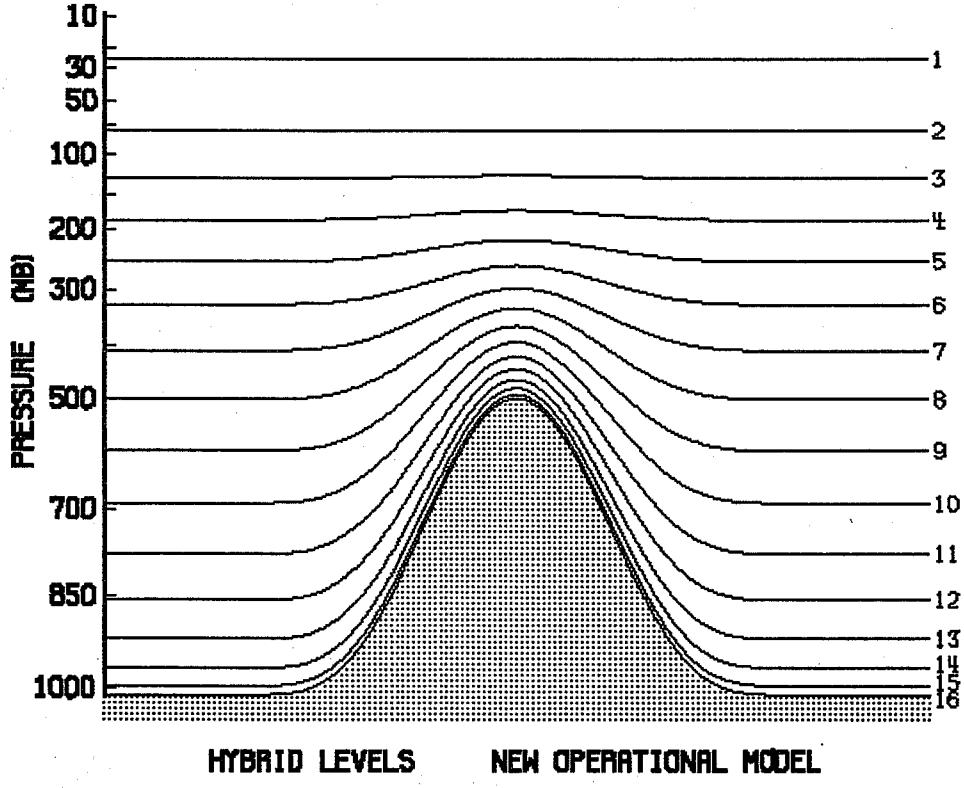

Fig. 1 Distributions of levels for the old and new operational models.

Simmons and Strüfing (1981) discuss a number of advantages of using a 'hybrid' vertical coordinate which resembles the usual sigma coordinate close to the ground, but which reduces smoothly to a pressure coordinate ($B_{k+1/2} = 0$) at stratospheric levels. Such a coordinate has been chosen for the operational application of the new model. 16 layers have been used, and in Figure 1 the levels at which the primary model variables are predicted are compared with the 15 levels of the former operational model. The additional level has been introduced near the surface to give a more consistent finite-difference scheme for this region,as discussed by Simmons (1983). Values of the $A_{k+1/2}$ and $B_{k+1/2}$ are specified in Table 1.

4. THE TIME-STEPPING SCHEME

In most respects the time-stepping scheme of the new model is as in the models developed earlier at the Centre, apart from a modification of the semi-implicit treatment of gravity-wave terms necessitated by the introduction of the more general vertical coordinate. Details of this change are again as discussed by Simmons and Strüfing (1981), and operational implementation has used an isothermal reference temperature of 300K and a reference surface pressure of 800 mb. However, in addition to this relatively minor change, a more significant modification has been developed following the observation by Robert (1981) that the timestep criterion in a conventional semi-implicit model is generally determined by the stability of the scheme for the horizontal advection of vorticity (and perhaps also, by implication, the horizontal advection of moisture).

The new scheme utilizes the fact that the predominant direction of the strongest atmospheric flow is zonal. The advection of vorticity and moisture is treated semi-implicitly, linearizing about advection by a zonally-uniform

zonal wind. Specifically,

$$\frac{1}{2\Delta t}\left\{X(t+\Delta t) - X(t-\Delta t)\right\} = X_T - \frac{u_o}{a\cos\theta}\frac{\partial}{\partial\lambda}\left\{X(t-\Delta t) + X(t+\Delta t) - 2X(t)\right\}$$

where X_T is the explicit tendency of X, X being either the vorticity or humidity variable, u_o is a height- and latitudinally-varying reference zonal wind, θ is latitude, λ is longitude, t is time and a is the radius of the earth. This equation is easily solved for $X(t+\Delta t)$ in Fourier space, although the use of integration by parts to compute spectral tendencies of vorticity necessitates the computation of values of $\partial u_o/\partial\theta$ as well as u_o for each latitude and model level. For the tests reported here and for the initial operational implementation, u_o was taken to be the zonal-mean of the instantaneous model zonal wind. It was changed early in December to be the arithmetic mean of the maximum and minimum zonal wind for timestep $t-\Delta t$, this having been found to give a slight increase in computational stability.

The scheme has made it possible to use timesteps between 25 and 50% longer than possible with the conventional semi-implicit treatment of gravity-wave terms alone. Figure 2 shows an objective verification of forecasts for the extratropical Northern Hemisphere for an extreme case in which strong flow in the polar stratosphere of the Southern Hemisphere resulted in the then operational grid-point model having to use a timestep of 10 minutes rather than its usual value of 15 minutes. For this example, use of the hybrid coordinate reduces the strongest winds in the model stratosphere over Antartica, since the top hybrid model level does not rise up over high ground, and with this coordinate a timestep of 12 minutes was possible with the grid-point model, and 15 minutes with the new T63 spectral model using a conventional semi-implicit scheme. Including the semi-implicit treatment of vorticity and moisture advection, a stable integration has been carried out using a timestep of 22.5 minutes, and figure 2 is an example of how no

Table 2 Anomaly correlations of 1000-200 mb heights for the extratropical Northern Hemisphere for 3-, 6- and 10-day forecasts for three cases using different models and timesteps.

Date	Forecast model	Timestep (minutes)	Height Anomaly Correlation Day 3	Day 6	Day 10
	Spectral	22.5	91.3	67.8	32.6
4 Feb	Spectral	18	91.5	67.8	33.1
	Grid-point	15	91.7	67.3	20.0
	Spectral	22.5	75.0	10.5	5.2
8 Aug	Spectral	18	74.4	10.1	2.5
	Grid-point	15	79.7	18.5	6.6
	Spectral	22.5	78.5	21.7	3.4
6 Sept	Spectral	15	78.6	20.1	0.4
	Grid-point	12	76.1	20.3	-7.6

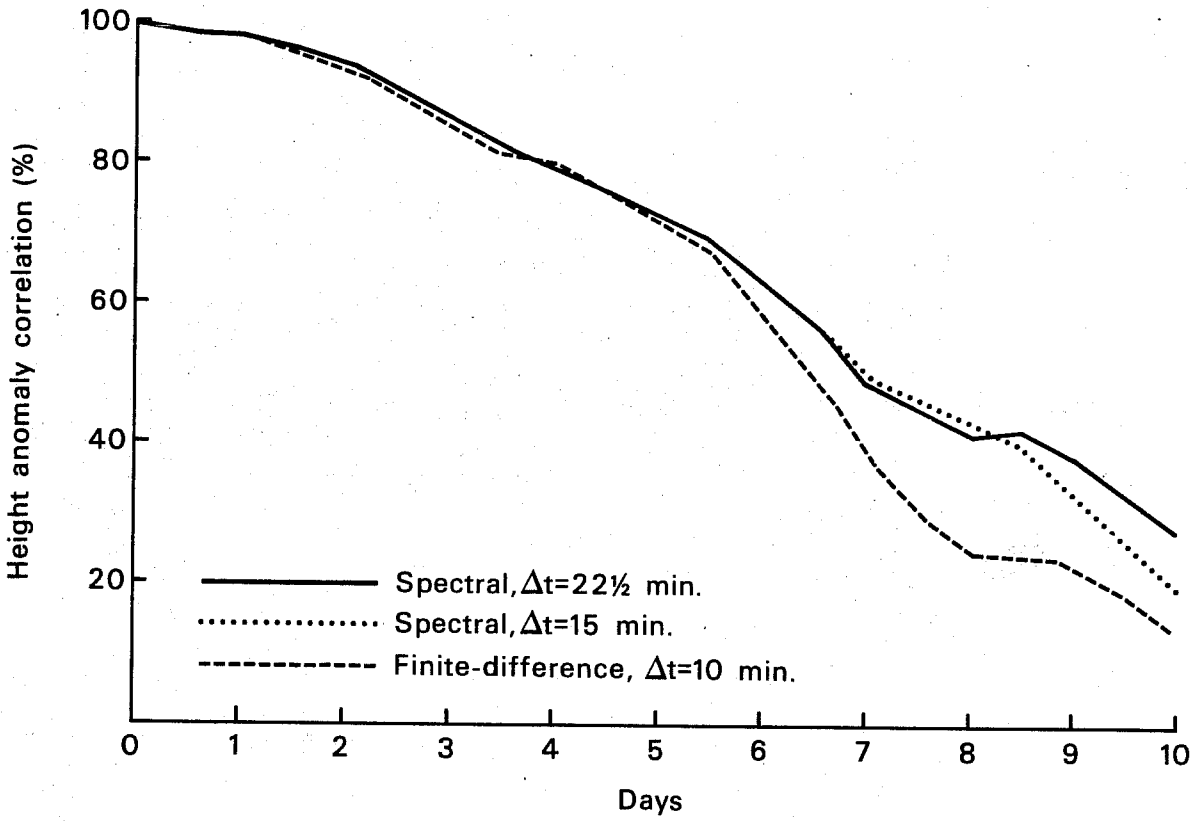

Fig. 2 Height anomaly correlations (%), calculated for the area from 20°N to 82.5°N using standard pressure levels from 1000 to 200 mb, plotted as functions of the forecast range in days. Results are shown for three forecasts (as labelled in the figure) from 4 October 1982.

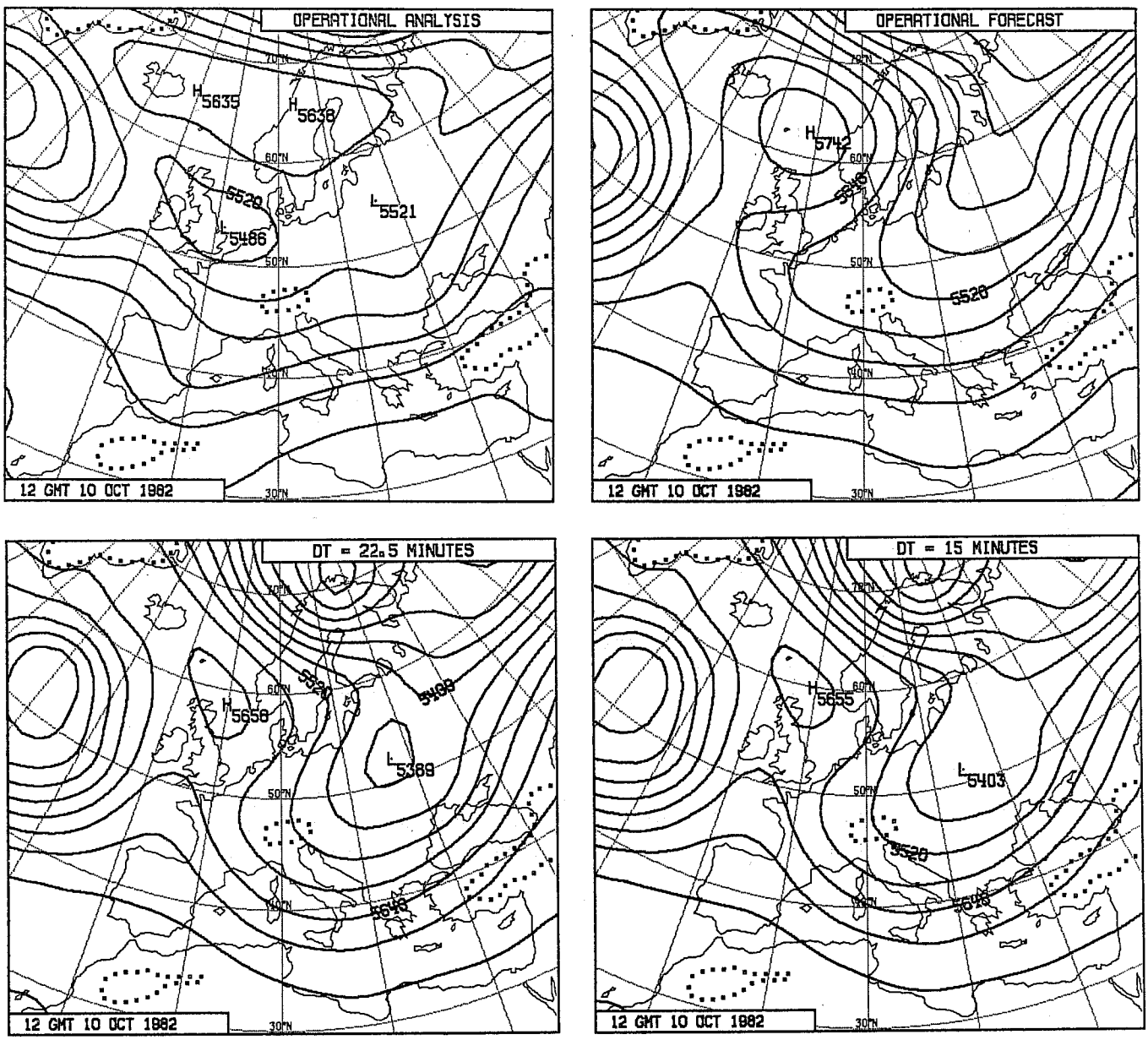

Fig. 3 Maps of 500 mb height (contour interval 60m) over Europe. The operational analysis for 10 October 1982 is shown in the upper-left panel and the 6-day operational (grid-point) forecast from 4 October carried out with a 10-minute timestep is upper right. Forecasts using the new model are shown for timesteps of $22\frac{1}{2}$ minutes (new time scheme, lower left) and 15 minutes (standard time scheme, lower right).

significant decrease in the objectively-measured forecast accuracy occurred as a result. Figure 3 shows corresponding 6-day maps of 500mb height over Europe, and it can be seen that differences between the two forecasts performed with the new model and different timesteps are quite negligible when compared with differences either between the new-model forecasts and the operational forecast, or between the new forecasts and the analyzed state of the atmosphere.

Similar conclusions have been drawn from three other cases, and some objective scores are shown in Table 2. A timestep of 22.5 minutes has been found to give stable forecasts for all cases tried using a grid-square mean orography, but has given instability in some tests using envelope orographies. In three particular cases studied with the new scheme, increasing the timestep has resulted in instability first developing in the region of strongest (and relatively zonal) flow in the tropospheric jetstream over the Western Pacific. The destabilizing effect of the envelope orographies appears to be an indirect one, through their tendency to enhance the speed of this jet. The new time scheme was used with a timestep of 20 minutes for the final tests of the new model and for its operational implementation.

One subsequent operational forecast, that from 19 August, has been unstable with the 20-minute timestep. The instability occurred late in the forecast, around day 8½, and as in unstable cases in previous years developed in the region of strongest flow in the polar stratosphere of the Southern Hemisphere. As an emergency operational procedure the forecast was successfully carried out to day 10 using a 15-minute timestep, and operational forecasts over the following 8 weeks were carried out with an 18-minute timestep before reverting to 20 minutes. The case has been the subject of some scrutiny, and the results seem of sufficient interest to justify recording here.

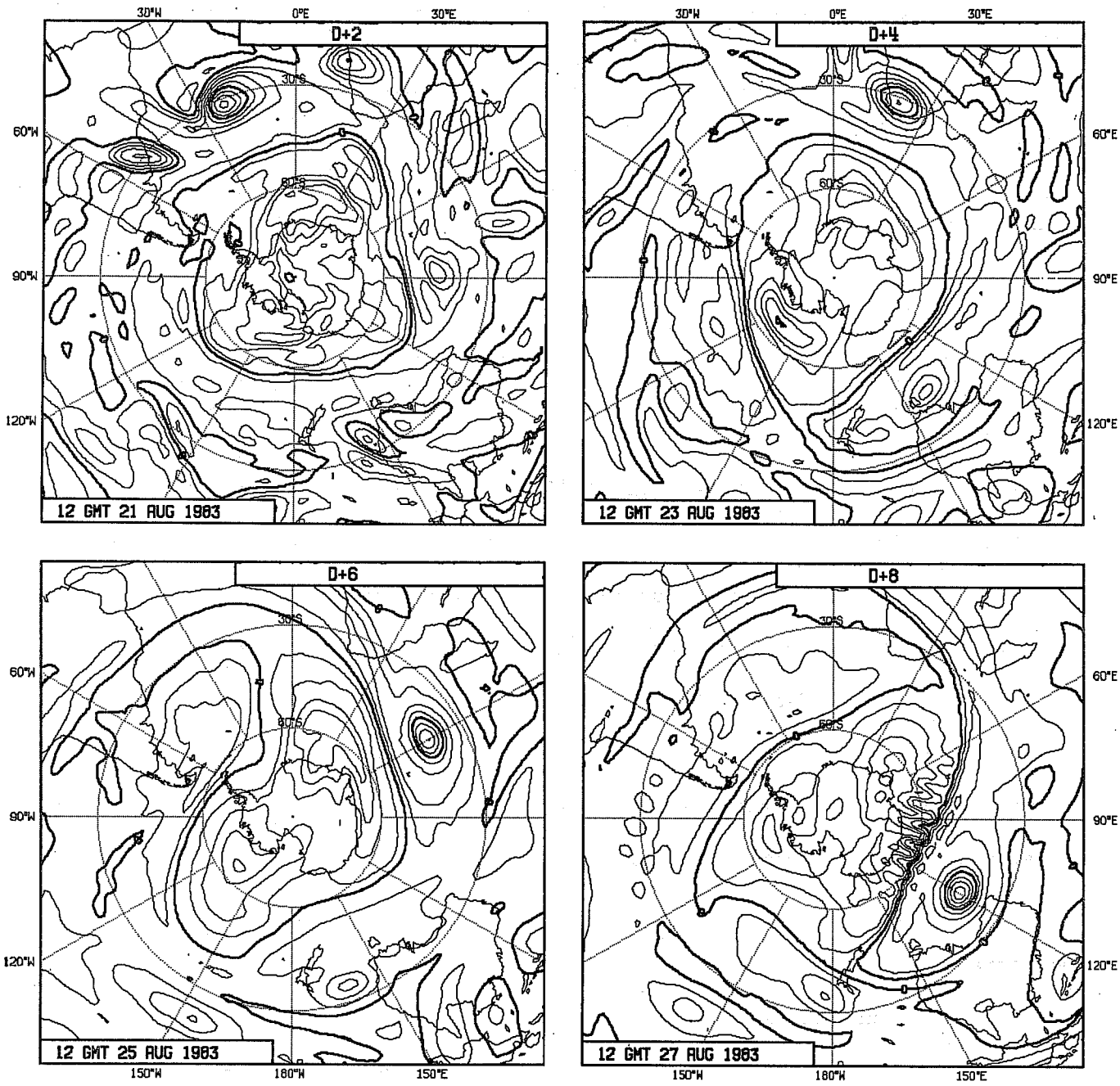

Fig. 4 Relative vorticity (contour interval $2 \times 10^{-5} s^{-1}$) at the top model level (25 mb) for days 2,4,6 and 8 of a forecast from the operational analysis for 19 August 1983. Maps are for the extratropical Southern Hemisphere, and over the course of the forecast exhibit a general reduction of small-scale noise present in the initial analysis. Heavy contours are drawn at an interval of $10^{-4} s^{-1}$, and the zero contour is marked in places. Values are negative in the polar region.

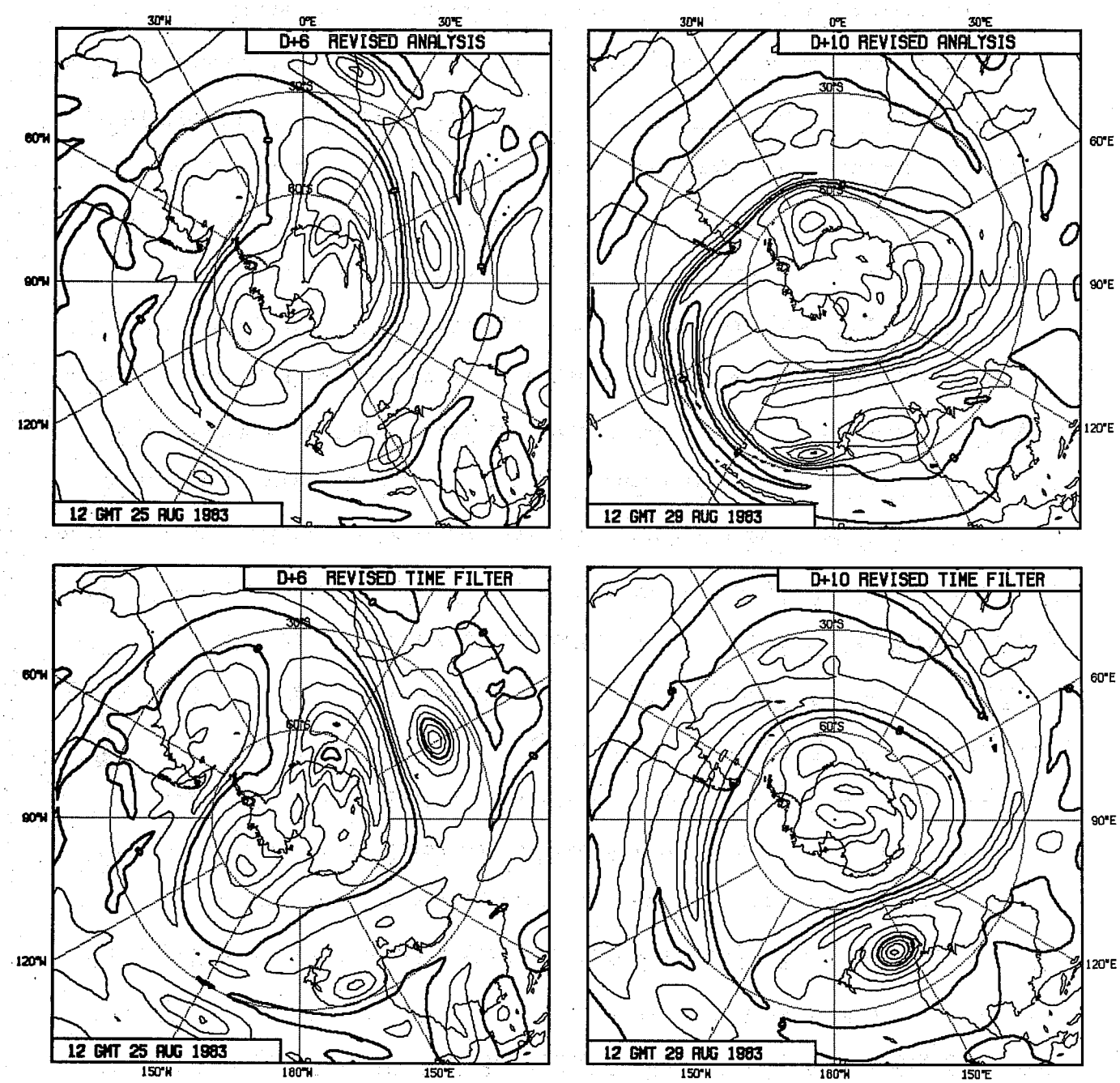

Fig. 5 Relative vorticity as in Fig. 4, but for day 6 and day 10 forecasts from a revised analysis in which an erroneous observation over South America was suppressed (upper), and from a forecast from the operational analysis using a larger coefficient for the time filter (lower).

A particular feature of the operational assimilation for the Southern Hemispheric stratosphere for 19 August was the acceptance of a clearly erroneous item of radiosonde data over South America. The analyzed relative vorticity at the top model level (25 mb) showed a very strong perturbation in the vicinity of the observation, and the subsequent evolution of this field during the course of the forecast, shown in Fig. 4, is strongly suggestive of an important role played by the erroneous datum in triggering the eventual destabilization of the forecast. The day 2 forecast presented in the upper left frame of Fig. 4 shows three centres of vorticity in the South Atlantic sector. Those over the coasts of South America and Africa subsequently decay, and do not concern us here. The relevant centre is that near 30°W, which originated from the erroneous datum, and has a positive maximum in excess of 1.6×10^{-4} s^{-1}, implying a locally positive absolute vorticity. It is located equatorward of the core of the polar-night jet, and by day 4 moves to be located over South Africa (Fig. 4, upper right), with little loss of amplitude. The lower panels of Fig. 4 show a continued eastward movement of the isolated centre, with again little change of amplitude. At day 6 the circulation associated with the centre begins to reinforce what appears to be a more natural strengthening of the jet to the south of the centre, and by day 8 the development of a small-scale instability in the vicinity of the jet maximum (near the heavy line denoting zero relative vorticity) is evident.

The above sequence, apart from demonstrating the ability of the model to maintain an isolated (albeit unrealistic and unwelcome) non-dispersive perturbation over an extended period of time, suggests that the origin of the instability can be traced back to the single erroneous observation over South America. This has been simply confirmed by repeating the analysis and performing a successful 10-day forecast with the erroneous stratospheric datum removed. The upper panels of Fig. 5 show the top-level relative vorticity

forecast for day 6 and day 10. At day 6 the forecast is very close to that shown in Fig. 4, apart from the absence of a strong, isolated centre at 60°E, although a weaker maximum has been seen to develop in a similar location. A very substantial development has occurred by day 10, a development suggestive of the "breaking" of planetary waves discussed by McIntyre and Palmer (1983), but no sign of computational instability is apparent.

Another feature of the unstable integration shown in Fig. 4 is the relatively slow development of the instability. When wind speeds exceed a computational stability limit it is commonly found that models fail within a few timesteps of the instability becoming noticeable. In the present case the model continued for more than 1½ days after small-scale wave development was first evident at the jet core. Closer examination showed the instability to arise in a computational (oscillatory in time) mode, and a successful 10-day forecast from the operational analysis has been found possible using a time-filter coefficient ($\nu/2$ in the nomenclature of Asselin, 1972) of 0.1, rather than the operational value of 0.06. Top-level relative vorticities at days 6 and 10 are presented in the lower panels of Fig. 5. At day 6 the field is almost identical to that shown in Fig. 4 for the unstable forecast. By day 8 (not shown) some small-scale noise develops much as is shown in Fig. 4, but with a significantly weaker amplitude, and Fig. 5 shows it to have disappeared by day 10. Still evident at this time is the remarkably persistent centre of positive vorticity initially located over South America, which after 10 days has reached southwest of Australia with little change in amplitude. Vorticity gradients differ noticeably in intensity in the two day-10 forecasts shown in Fig. 5. Further experimentation has shown this to be a consequence of the differences in analysis rather than the differences in time scheme.

Use of the larger time filter in this and other tests has been found to have negligible impact on tropospheric forecast quality, and an operational change to the larger value was made early in December.

5. ADDITIONAL CHANGES TO THE FORECASTING SYSTEM

Although the basic types of parameterization scheme are unchanged in the new model, the existing routines have been reprogrammed to allow for the new vertical coordinate and to incorporate the new coding practices discussed below. The oportunity was also taken to introduce a number of revisions in the detailed formulation of the schemes. Among these are a distinction between the latent heats of vaporization and sublimation, and a generally more consistent treatment of moist processes, including use of separate specific heats for dry air and water vapour. The latter was also introduced into the energy-conversion term of the unparameterized temperature equation, thereby removing an inconsistency present in the Centre's original grid-point and spectral models, which recognized the difference between temperature and virtual temperature but not the numerically as important difference between the specific heats. Other changes to the parameterization included some modifications of the radiation scheme, and the introduction of a more stable algorithm for the time-stepping of the equations for surface fields.

For the first operational application of the new model in data assimilation it was impractical to change the code of the analysis to accept a first guess on the model's Gaussian grid and evaluate the resulting analysis on this same grid. Thus the model post-processing code was adapted to interpolate fields between the model grid and the regular 1.875° grid of the analysis. The post-processing itself has been reprogrammed, and the options for vertical interpolation expanded. Use of 'tension splines' (Cline, 1974) has been found to give improved results for most fields, and has been introduced operationally. Routines to perform the vertical interpolation between model

levels and the standard pressure levels of the analysis have also been rewritten, and tension-spline interpolation has also been introduced into the calculation of the pressure-level first-guess. The code of the diabatic nonlinear normal-mode initialization has been rewritten for the general vertical coordinate and basic spectral representation, and incorporated within the model itself. Initialization is thus performed as an option at the start of a model run.

The new model, post-processing and model/analysis interfaces have been coded using new programming standards and techniques. A set of memory-management routines (Gibson, 1983) has been provided to facilitate repeated use of specific areas of memory for different purposes during the execution of a programme, and this has allowed meaningfully-named multi-dimensional arrays to be used throughout the code. Specific rules have been laid down for the FORTRAN coding, including conventions for the use of comment cards to aid automatic extraction of documentation for each subroutine. Modularity has been an objective of the programme design, and flexibility has been incorporated into the input/output scheme to allow effective use of the alternative secondary storage devices of the CRAY X-MP computer.

The net time taken for the operational 12Z analysis, initialization and 10-day forecast is currently of the order of 10% longer than taken by the former operational grid-point model with its usual 15-minute timestep, although the reduction in timestep necessitated by introduction of the envelope orography, and the greater stability of the new model in some cases of strong stratospheric flow have to be noted when making such comparisons. The additional computing cost of the hybrid vertical coordinate, the extra model level, more complex parameterizations and overall flexibility has been

covered by the use of the more efficient time scheme. Some further optimization of the model is also likely.

6. THE NEW OROGRAPHY

Diagnostic and barotropic model studies reported by Wallace et al.(1983) have suggested that the use of a grid-square mean orography significantly underestimates the orographic forcing of the synoptic and larger-scale winter-time flow in the Centre's grid-point model forecasts. These studies have led to prediction experiments, some of which are described by Wallace et al., using an envelope orography formed by adding to the mean orography twice the standard deviation of the actual orography over the grid square, this being computed from a very high resolution (10') data set made available by the US Navy through NCAR. Some significant improvements in the accuracy of winter forecasts have been found, amounting to a mean increase in medium-range predictability of the order of 6 to 12 hours. The rate of growth of some systematic errors was also substantially reduced.

The above experiments also exhibited a deterioration of the short-range forecasts, and some diagnostics were suggestive of an overestimation of orographic forcing using a 2 standard-deviation envelope, a suggestion reinforced by limited-area model forecasts of Alpine lee cyclogenesis at higher resolution (Dell'Osso, 1983). Thus prior to selecting an orography for use with the new model, a series of one-week data assimilations were performed, these using the grid-point model since the new model could not at the time be used in data assimilation. These experiments used orographies based on 1, $\sqrt{2}$ and 2 standard-deviation envelopes, and the operational analyses using a mean orography were also available. Forecasts with the new model were performed for each orography, and confirmed the general benefit of use of an envelope. Although the best objectively-measured performance was

achieved using 2 standard deviations, the $\sqrt{2}$ standard-deviation orography did not give significantly poorer results, and was chosen as the basis for the new operational orography. However, the use of envelope orographies generally resulted in an increase in the number of observations from coastal stations discarded by the analysis on the basis of the difference between the height of the station and that of the model orography. The basic spectrally-fitted envelope orography was thus modified in an iterative procedure which restored sea points (points with >50% of the grid-square sea) to zero height between successive spectral fits of the orography as defined on the model's Gaussian grid.

A sequence of new-model forecasts has been carried out using this orography and the grid-square mean orography, for the week 19-25 December 1982. Anomaly correlations for the extratropical Northern Hemisphere are compared in the scatter diagrams presented in Fig. 6. As in the corresponding results from grid-point model forecasts using a 2 standard-deviation envelope (Fig. 19, Wallace et al., 1983), there is a deterioration in the one-day forecasts due to use of the envelope orography, but a very clear benefit in the medium range, improvement occurring in every forecast at the 4- and 7-day range. The improvement here is generally larger than found by Wallace et al. for a 21-day sequence of forecasts, and at least for this one particular week it appears due to a greater sensitivity of the spectral model to the envelope orography. Predictability measures from grid-point and spectral forecasts are compared in Table 3, and it is clear that for the period in question the (relatively poor) spectral forecasts were on average substantially improved by use of the higher orography, whereas a more modest improvement is seen in the grid-point forecasts. General conclusions cannot, of course, be drawn from such an experiment, but repetition of one of the cases examined by Wallace et al. has given a similar result.

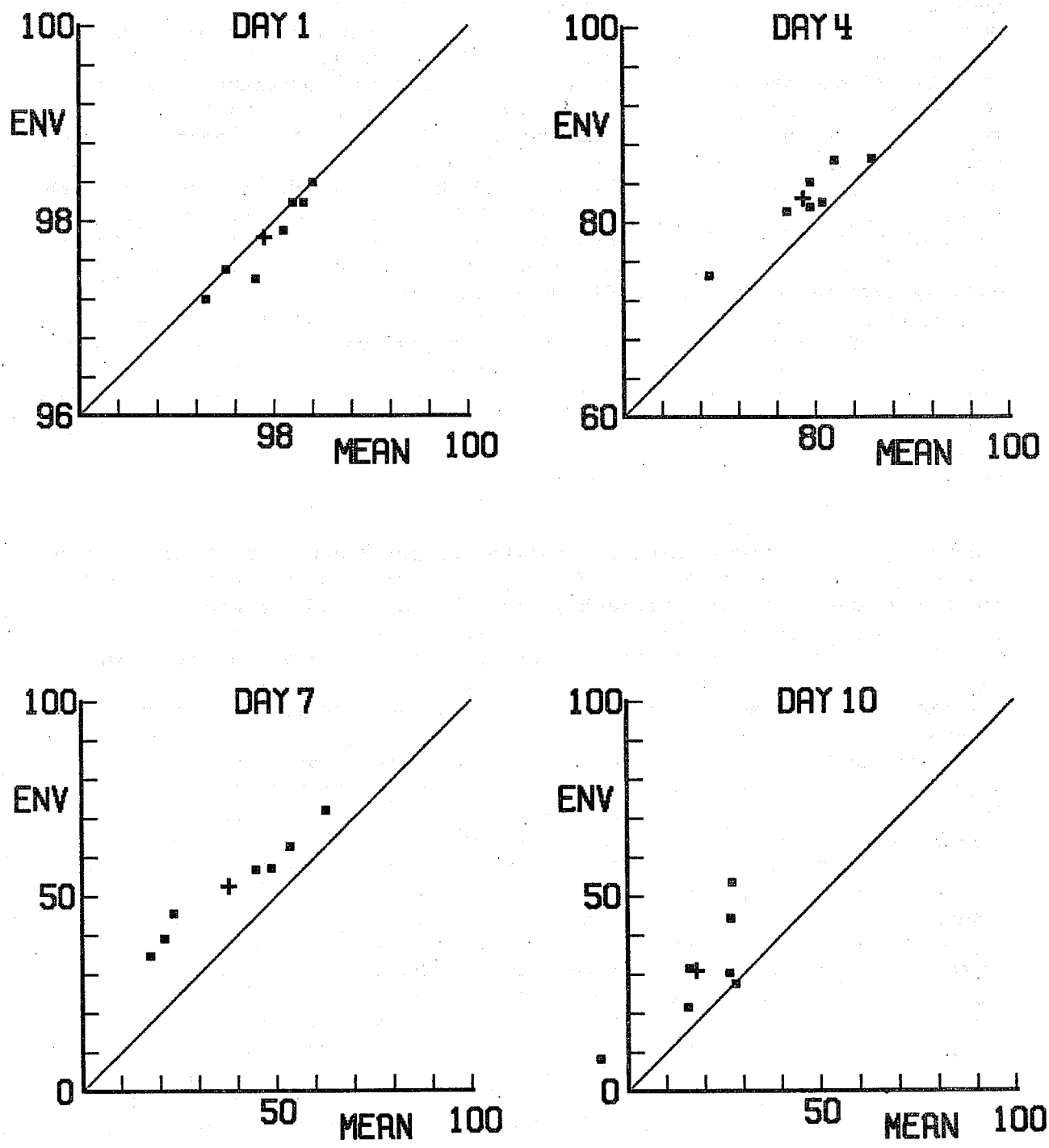

Fig. 6 Height anomaly correlations (1000-200 mb, 20^{o}-82.5^{o}N, %) from 1-, 4-, 7- and 10-day forecasts using mean and envelope orographies.

Table 3 Predictability, measured by the forecast time (in days) at which the anomaly correlation of 1000-200 mb height for the extratropical Northern Hemisphere falls below 60%, for forecasts from Dec 1982 using mean and envelope orographies, and the then operational grid-point model and the new spectral model.

	Grid-point		Spectral	
Date	Mean	Envelope	Mean	Envelope
19 Dec	6.8	6.7	6.0	7.1
20 Dec	6.1	6.2	5.5	6.2
21 Dec	5.9	5.7	6.1	6.1
22 Dec	5.6	5.5	5.1	5.1
23 Dec	5.0	6.3	4.4	5.4
24 Dec	6.5	7.2	6.3	7.5
25 Dec	7.8	8.2	7.2	7.8
AVERAGE	6.2	6.5	5.8	6.5

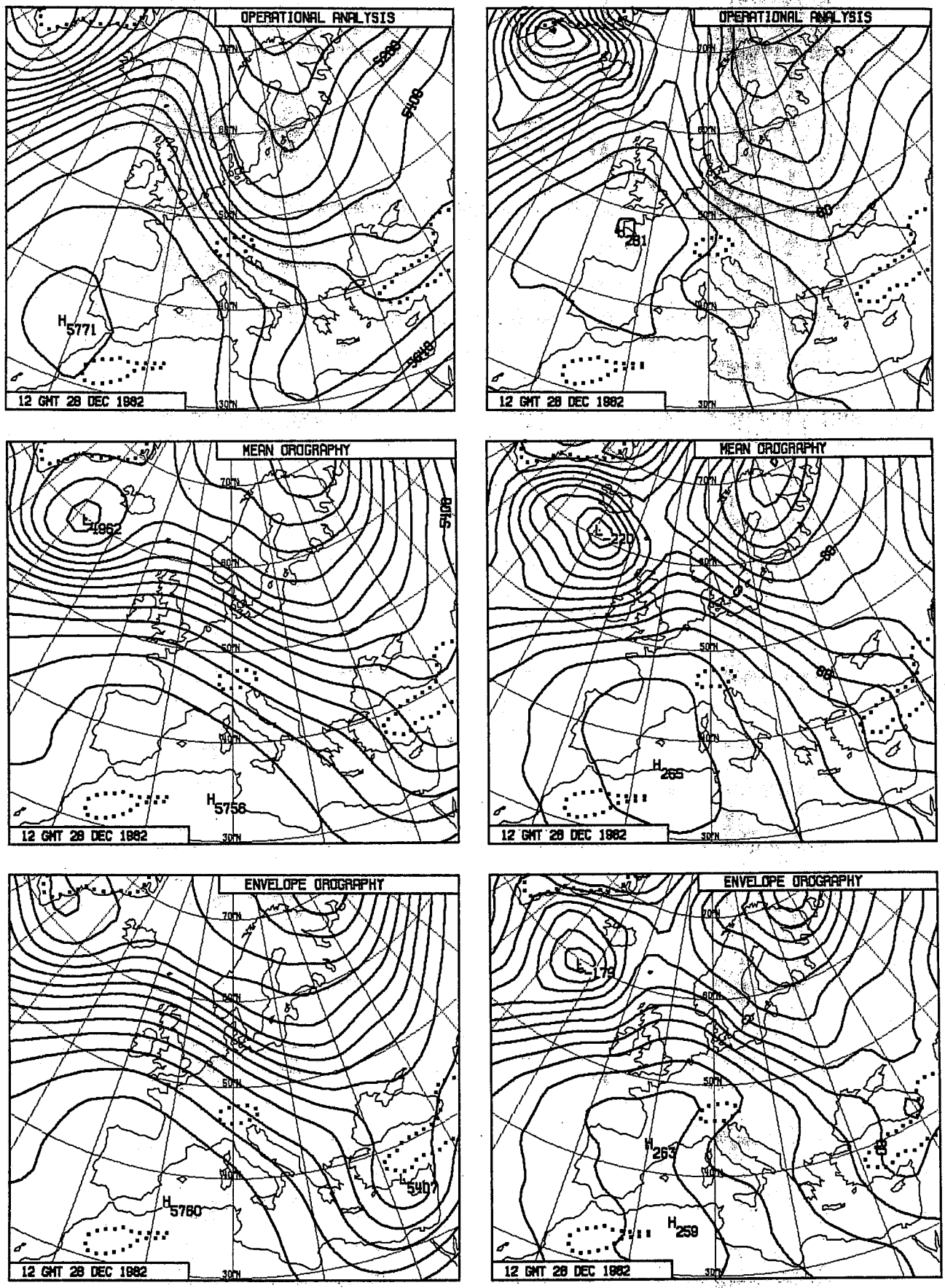

500 mb

1000 mb

Fig. 7 Maps of 500 mb height (left, contour interval 60m) and 1000 mb height (right, contour interval 40m) from operational analyses for 28 December 1982 (upper) and from 5-day forecasts from 23 December using mean (middle) and envelope (lower) orographies.

5-day forecasts of 500 and 1000mb height over Europe are compared with verifying analyses in Fig. 7 for new-model forecasts using mean and envelope orographies. The case chosen, 23 December, is distinguished as clearly the poorest in the results for day 4 shown in Fig. 6, and objective scores were improved substantially in this case by the change to the envelope orography. Serious deficiencies are evident in the 5-day forecast charts shown in Fig. 7, but the erroneous eastward displacement of the 500 mb trough over the Eastern Mediterranean is clearly less using the envelope orography, and the surface pattern in the lee of the Alps is better. An improvement may also be seen in the vicinity of Iceland.

Some other examples of forecast improvements which may well be due to the change in orography will be shown in our subsequent discussion of the results of the final pre-operational trial of the new forecasting system. A number of minor deficiencies have, however, been noted in relation to the iterative modification of the spectral fit introduced to reduce the height of the model orography near coastlines. An alternative orography, based on a direct spectral fit to a $\sqrt{2}$ standard-deviation envelope, but with a sub-grid variance taken into account only over land points, has been satisfactorily tested, and introduced into operations at the end of January 1984.

It is important to note that the preceding results all apply to winter forecasts. Some remarks on the performance of the envelope orography in summer predictions will be given in Section 10 in the context of the overall operational performance of the new forecasting system.

7. HORIZONTAL DIFFUSION

The form of horizontal diffusion adopted initially for the new model is a simple ∇^4 operator applied to the model's predicted upper-air fields, as in

the Centre's original spectral model. Initial tests were carried out using the coefficient of $7 \times 10^{14} m^4 s^{-1}$ used previously, but as a small amount of roughness was noted in precipitation fields, a series of 8 forecasts (using the mean orography) was repeated using coefficients of 2×10^{15} and $4 \times 10^{15} m^4 s^{-1}$. Objective verification showed a quite small, but not entirely negligible, sensitivity of the large-scale forecasts to the choice of coefficient. When carried out for the Northern Hemisphere it generally favoured use of 4×10^{15}, although the value of 7×10^{14} was preferred for the Southern Hemisphere.

An objective verification for the most sensitive Northern-Hemispheric forecast is shown in Fig. 8, and day 6 forecasts of 1000 mb height over Europe are compared in Fig. 9. It is clear that the three forecasts exhibit the same major synoptic-scale error, and with weaker diffusion there is a deepening of the erroneous low north of the Black Sea which contributes to the poorer verification found using the smaller diffusion coefficients. However, the phase of the short-wave trough to the south-west of the United Kingdom is better in the forecasts with lower diffusion.

In the absence of any clear-cut evidence, the coefficient of 2×10^{15} was chosen for the operational implementation of the new model, although further study has been stimulated by two features of the model's subsequent performance. The first was a tendency for excessive precipitation to occur over some mountainous areas in summer forecasts. A similar deficiency had earlier been encountered in a more marked form when the then operational grid-point model was first used with a grid-square mean orography, but was not obvious in spectral forecasts using a similar orography. A modification to the diffusion similar to, though simpler than, that developed for the grid-point model by Burridge (personal communication) has thus been tested.

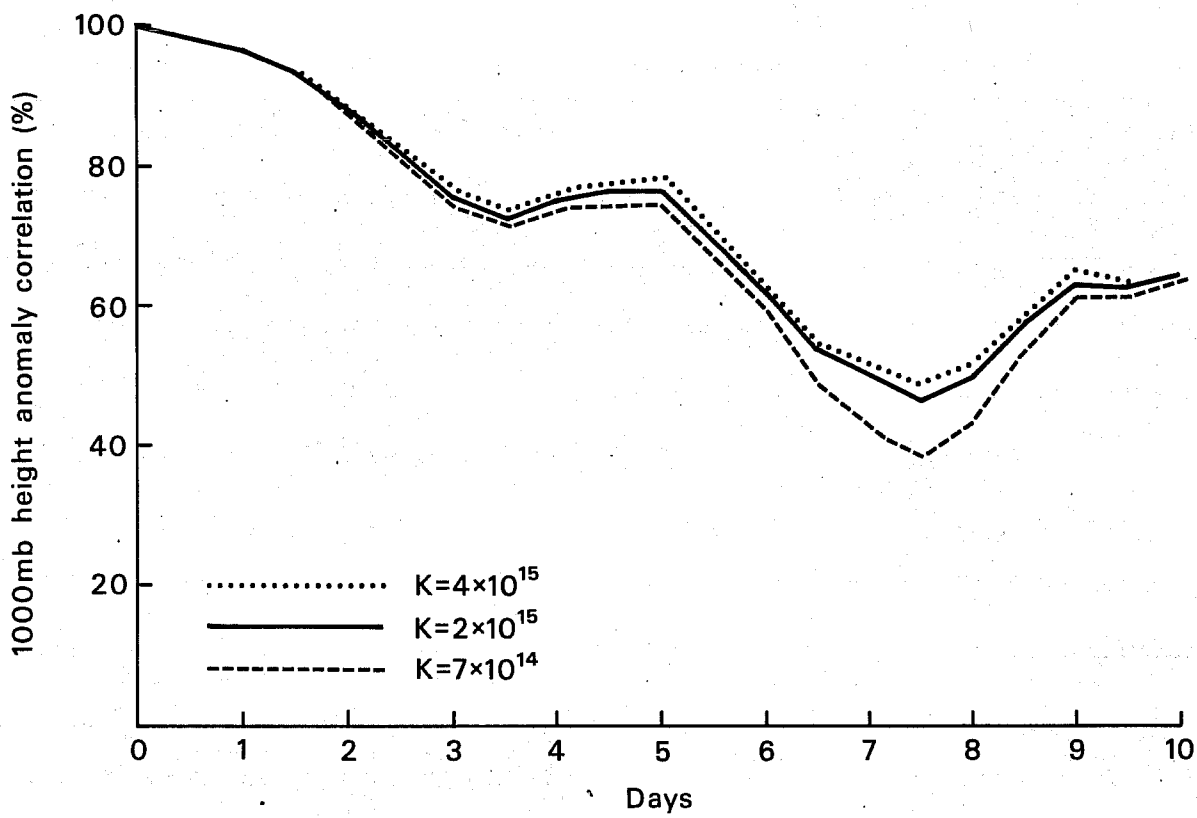

Fig. 8 1000 mb height anomaly correlations for the extratropical Northern Hemisphere for three forecasts from 28 February 1982 using different diffusion coefficients as specified in the figure.

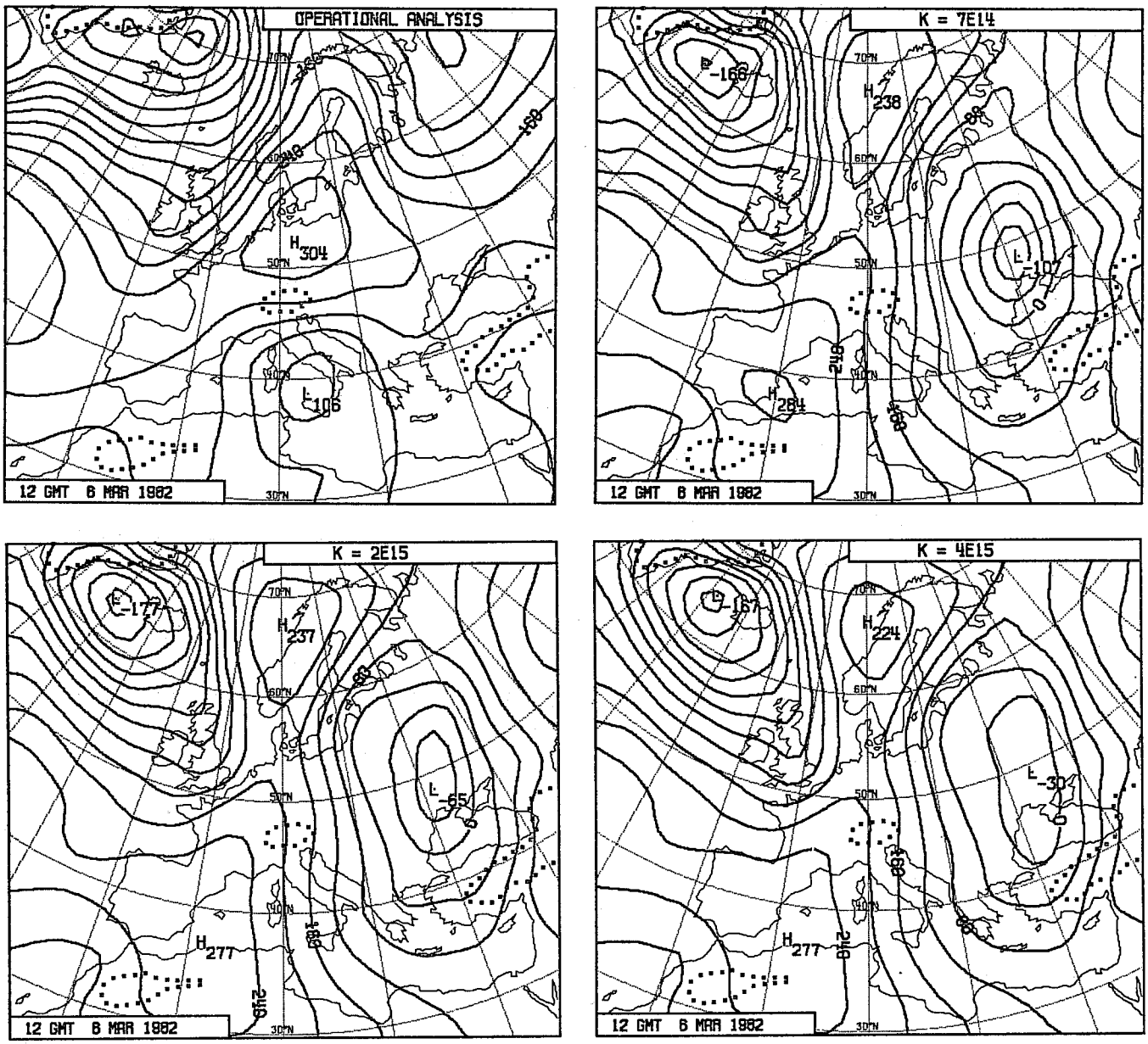

Fig. 9 Maps of 1000 mb height (contour interval 40m) for 6 March 1982. The operational analysis is shown in the upper-left panel, while the other panels show day-6 forecasts using diffusion coefficients of 7×10^{14} m s^{-1} (upper right), $2 \times 10^{15} m^4 s^{-1}$ (lower left) and $4 \times 10^{15} m^4 s^{-1}$ (lower right).

Horizontal diffusion is applied not to the temperature T alone, but rather to

$$T - \left(p_s \frac{\partial p}{\partial p_s} \frac{\partial T}{\partial p}\right)_{ref} \ell n p_s$$

where $(\ )_{ref}$ denotes reference values varying only with the model level. The chosen values are based on the standard ICAO atmosphere. This modified scheme approximates the diffusion of temperature on pressure surfaces rather than model coordinate surfaces, and vanishes at levels where the model coordinate reduces to a pressure coordinate, since $\partial p/\partial p_s = 0$ at such levels. The tests indeed showed a reduction of the excessive rainfall, and the scheme was introduced into operational forecasting at the end of August.

The second relevant feature of the operational performance of the new model is a tendency for pronounced wavetrains to develop occasionally in the vertical velocity field. These emanate from locations of strong convective activity, and occur on scales close to the smallest that can be resolved by the model. Preliminary tests have shown that they may be removed by increasing by a factor of 10 the diffusion coefficient for either divergence or temperature. This gives in some cases a band of rising motion in the same location as the wavetrain, with a largely unchanged pattern of accumulated precipitation, whereas in other cases a more localized area of rising motion and precipitation is found. Pending further investigation of the nature of these wavetrains, cases exhibiting them are being used to test alternative formulations for the horizontal diffusion and the impact of higher resolution.

8. REPRESENTATION OF SURFACE PRESSURE

In common with most spectral models, the new operational model has been based on a spectral representation for the logarithm of surface pressure, rather than surface pressure itself. This has some computational advantage for a

sigma-coordinate model, but the advantage disappears when the more general coordinate described in Section 3 is used.

Indeed, during development of the new model three advantages have been found to result from use of surface pressure rather than its logarithm as the basic prognostic variable. These are:

(i) Stability of the semi-implicit time scheme. Simmons and Strüfing (1981) discuss how use of p_s rather than $\ell n(p_s)$ gives less likelihood of computational instability of the semi-implicit scheme for gravity-wave terms when a hybrid coordinate is used.

(ii) Conservation of mass. Use of p_s results in formal mass conservation by the model. This is because the resulting equation for the tendency of p_s involves basic spectrally-represented fields in at most quadratic products, and the conservation properties of the continuous equations are thus preserved by the spectral technique. This holds even for a semi-implicit time scheme since the global means of the divergence fields which appear in the semi-implicit correction vanish identically. Non-conservation of mass due to use of ℓnp_s in the operational forecast model is quite insignificant on the 10-day time scale, but a mass loss equivalent to a global surface-pressure fall of 2.5mb has been found in a 10-year integration of the Centre's original sigma-coordinate spectral model at resolution T21 (Cubasch, personal communication).

(iii) Realistic surface-pressure tendency calculations. Initialized datasets for the new model yield a smooth variation of surface pressure in time, but if $\ell n(p_s)$ is used as the basic variable the directly-computed (and thus aliased) instantaneous tendency of p_s shows small-scale noise near steep mountain slopes. This does not occur if p_s itself is used as the variable

represented by the truncated spectral expansion. This problem is currently only a diagnostic one, but might require attention if a future data assimilation system were to make direct use of surface pressure tendency data.

One clear disadvantage of using p_s as the basic variable has been found. Calculations using an idealized temperature distribution which was a function of pressure alone have shown a substantial increase in error in the computation of pressure gradients in the vicinity of steep mountains. In practice, initialization compensates for this by introducing small-scale wave structures into the temperature field, with maximum amplitudes of about 1K over the Himalayas and Andes. This disadvantage is a consequence of a much stronger aliasing in the computation of the term $R_d T_v \nabla \ell n p$ (cf. equations (93) and (94) of our earlier presentation of the spectral technique). An alternative model formulation has been developed which has been shown in the idealized calculations to alleviate the problem by use of a different prognostic variable for the temperature field. Details will be reported elsewhere should more extensive testing prove successful.

9. PRE-OPERATIONAL TRIALS

In addition to the tests reported in preceding sections, two trials of the new model have been carried out prior to its operational implementation. The first tested the impact of the model in isolation. Thirteen forecasts at weekly intervals from the winter of 1982/1983 were performed from initialized datasets produced using the then-operational grid-point model in the data assimilation. As in the other tests that have already been described, the analyses were interpolated to the new model levels and spectrally fitted. No further initialization was performed. The forecasts used the same grid-square mean orography as in the assimilating model, and verification was

performed against the initialized operational analyses. This set of forecasts will be referred to as the 'winter tests', and some results have already been discussed in the preceding paper comparing spectral and grid-point forecasts.

The second trial comprised a quasi-operational run of 19 days immediately prior to the actual operational changeover. In this case the new model was incorporated in the data assimilation, and the envelope orography was also used. Forecasts were run each day, but 4 of the 19 were terminated before 10 days because of shortages of computing time. This trial was the first full test of the data assimilation system for the new model, and technical problems led to use of climatological rather than analyzed sea-surface temperatures for the first few days, and to the discarding of about half the Southern-Hemispheric pseudo-observations (PAOBS) for much of the period. These problems are unlikely to have influenced significantly the results to be discussed here. To avoid any small biases, forecasts made by a particular model were verified where possible against (initialized) analyses produced using the same model. This second trial of the new model will be referred to as the 'parallel run'.

A convenient way of illustrating the objectively-measured difference between two sets of forecasts is through 'predictability' graphs (Girard and Jarraud, 1982). For each case, the forecast time at which an objective measure (assumed for the purposes of explanation to decrease with decreasing forecast accuracy) first falls below a certain value is computed, here using linear interpolation between scores available daily for the parallel run. These times are averaged over the forecasts performed by each model, and the difference of this average gives the difference in time at which a given level

of forecast accuracy is on average reached. Curves may be plotted by calculating averages for a range of accuracies lying above a limit below which all predictions fall at some time during the 10-day forecast period.

Such graphs have been shown in Fig. 24 of the preceding paper for the winter tests, and corresponding results from the parallel run are shown here in Fig. 10. At 1000 mb the improvement in medium-range predictability is much the same as the 12 hours found for the winter tests, but in this case improvement is more evident earlier in the forecast range. This occurs despite the generally detrimental effect of the envelope orography on short-range forecasts found previously, and it is most likely a consequence of the benefits of having the new model and consistent initialization in the data assimilation cycles. At 500mb an improvement in predictability occurs which is much more substantial than found for the winter tests, this amounting to as much as one day at the 50% level. This is consistent with earlier experimental results, for example those of Wallace et al.(1983), which show a more pronounced impact of the envelope orography on forecast accuracy at 500mb than at the surface. However it must again be stressed that the results shown here are for one particular rather limited period.

The objective results obtained using anomaly correlations are generally confirmed using other measures, though emphasis differs somewhat. For example, Figs. 11 and 12 show results for a measure based on the standard deviation of each model forecast normalized by the standard deviation of the corresponding persistence forecast. These results are presented not as predictability curves but as simple averages over all forecasts in order to show the full forecast range.

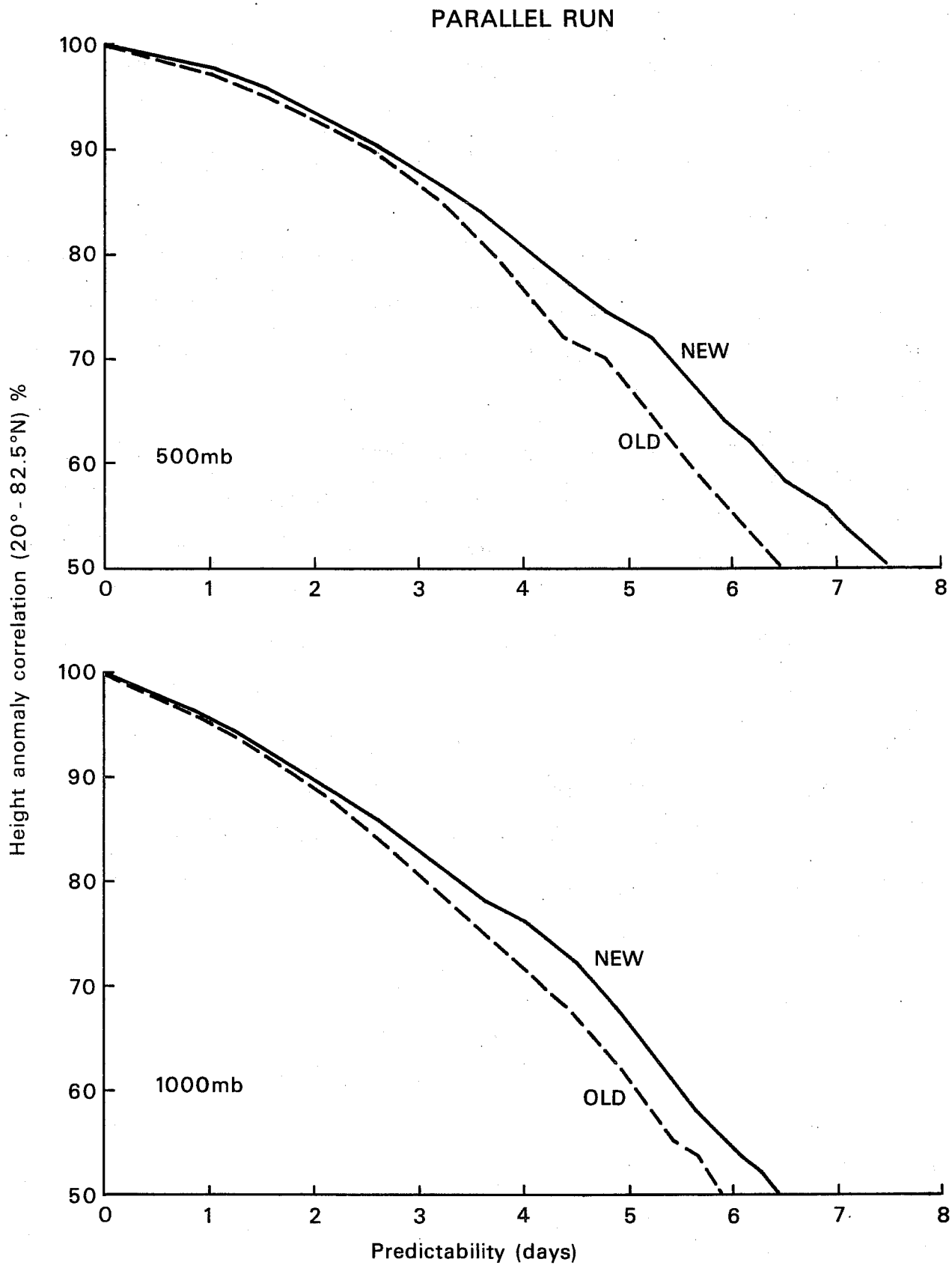

Fig. 10 Predictability graphs based on anomaly correlations of 500 mb height (upper) and 1000 mb height (lower) for the extra-tropical Northern Hemisphere. Results are based on 15 cases from the "parallel run" between 2 and 20 April 1983. "NEW" and "OLD" denote respectively the new spectral, hybrid-coordinate model, and the former operational grid-point model.

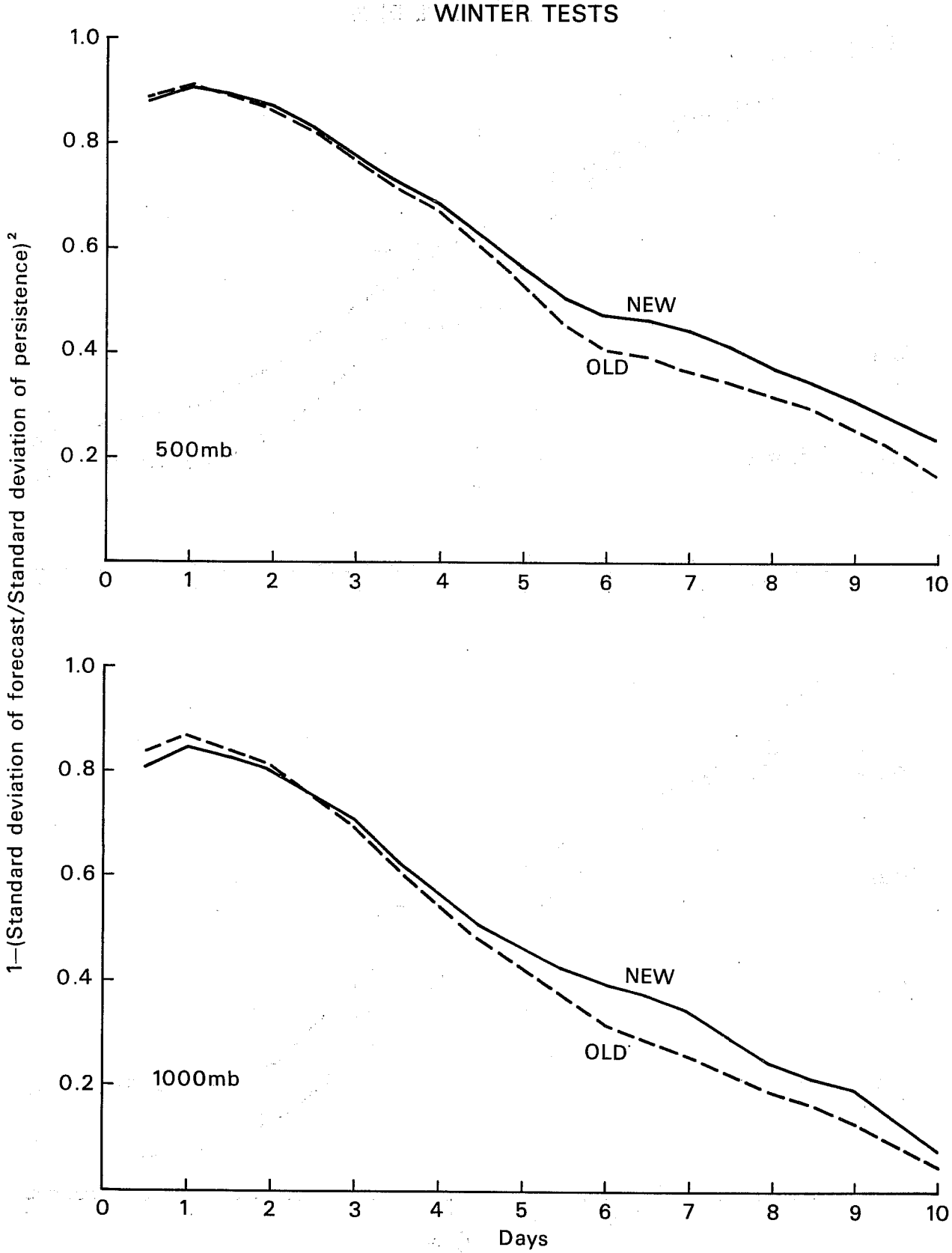

Fig. 11 A measure of forecast accuracy based on standard deviation computed over the extratropical Northern Hemisphere for 500 mb height (upper) and 1000 mb height (lower), averaged for the 13 forecasts compared in the "winter tests".

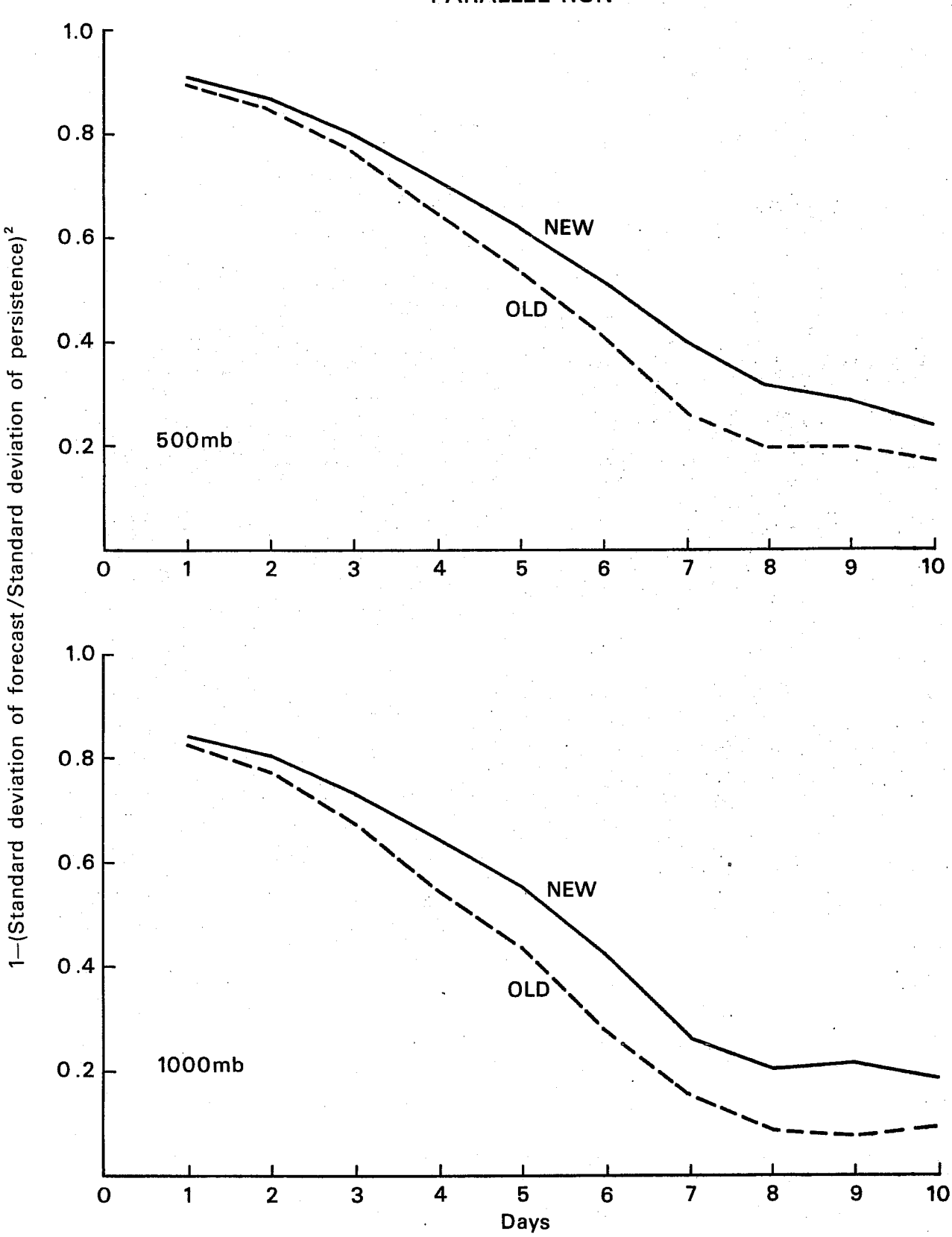

Fig. 12 As Fig. 10, but comparing means based on all forecasts performed during the "parallel run".

Winter tests

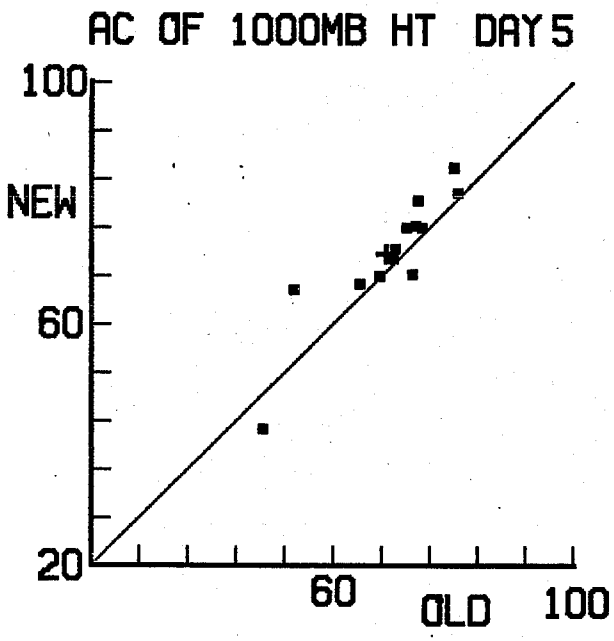

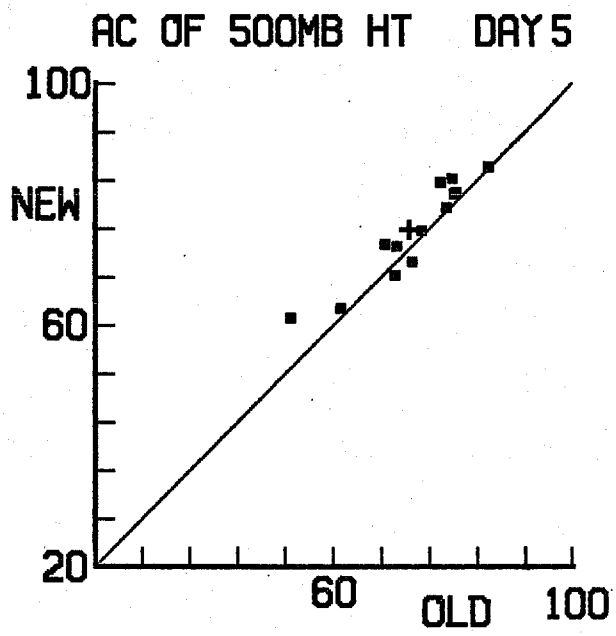

Parallel run

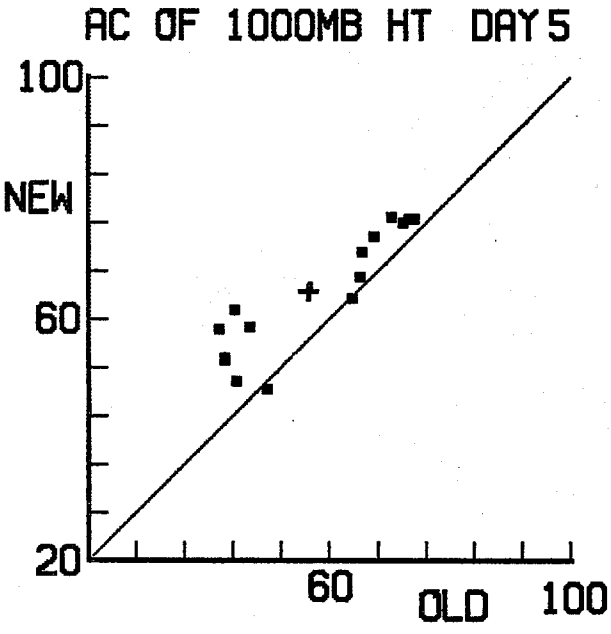

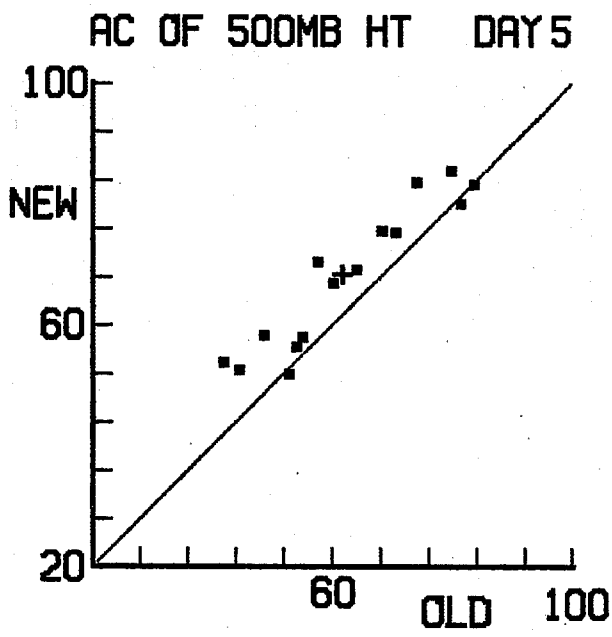

Fig. 13 Anomaly correlations of 1000 mb height (left) and 500 mb height (right) for the extratropical Northern Hemisphere for all day-5 forecasts from the "winter tests" (upper) and the "parallel run" (lower).

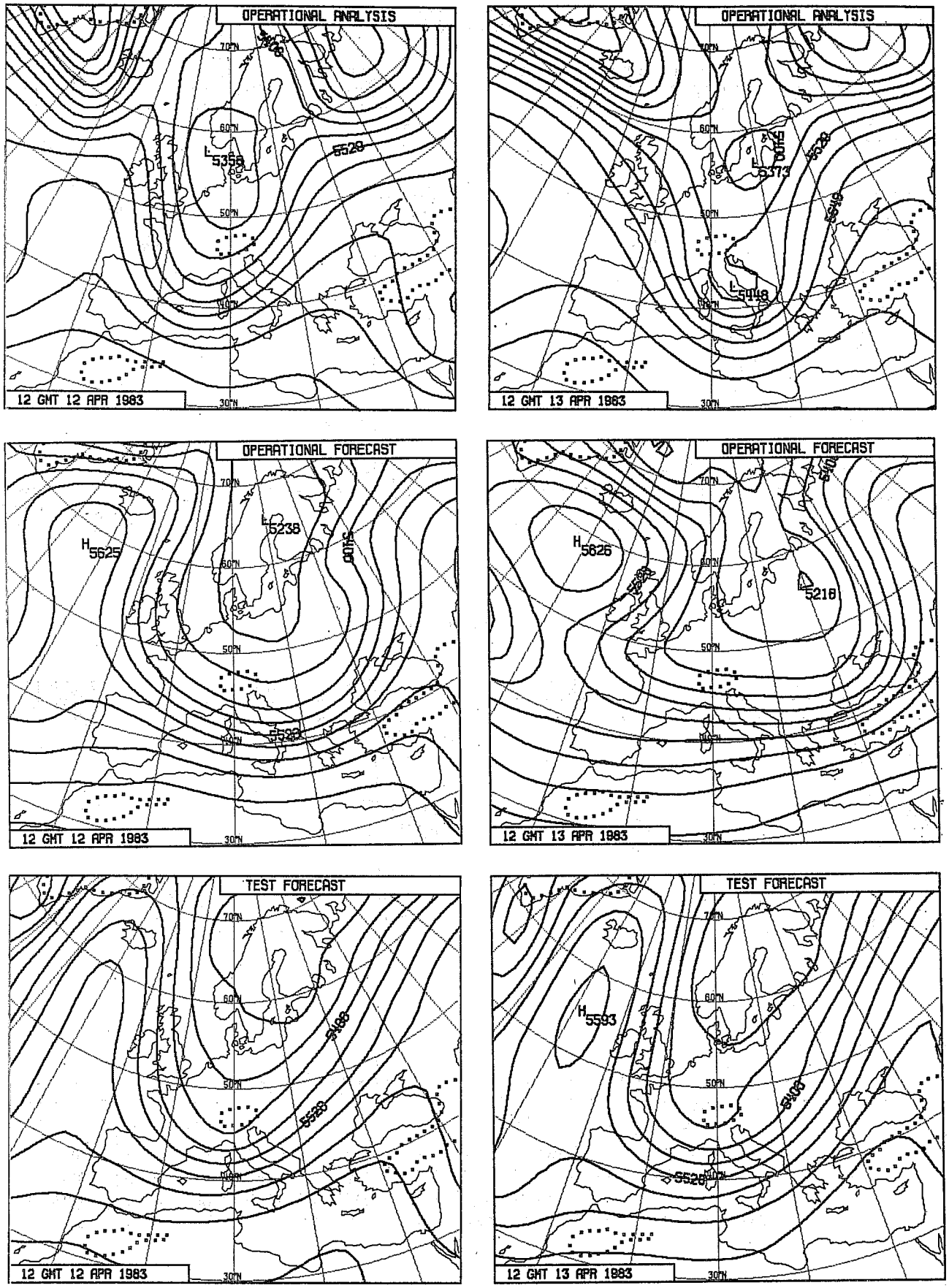

Fig. 14 Maps of 500 mb height (contour interval 60m) from operational analyses for 12 (upper left) and 13 (upper right) April 1983, and for 5-day (left) and 6-day (right) forecasts verifying on these dates. The middle panels show the operational (grid-point model) forecasts, and the lower panels the test forecasts using the new system.

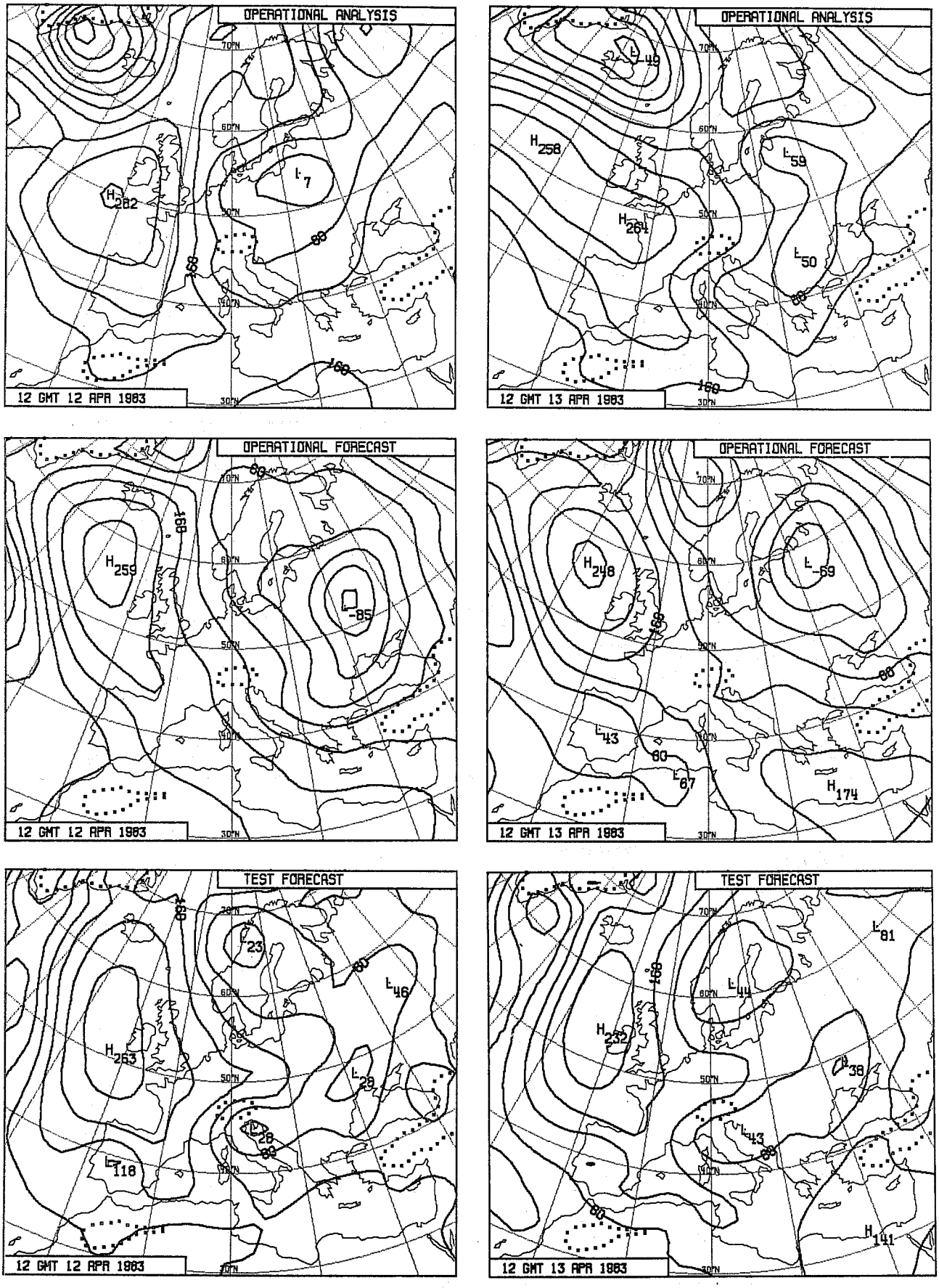

Fig. 15 As Fig. 13, but for 1000 mb height (contour interval 40m).

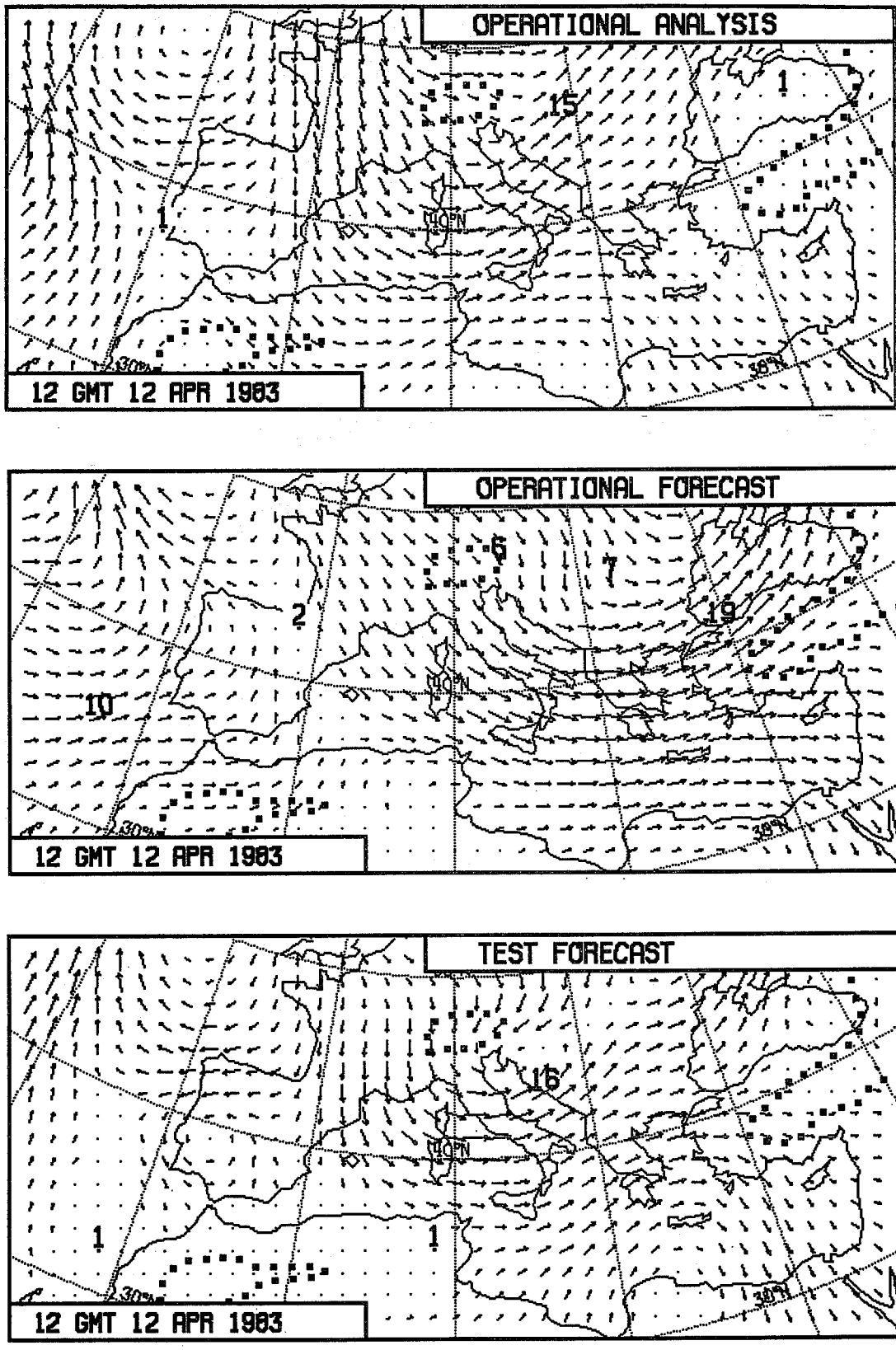

Fig. 16 The 850 mb wind analysis over Southern Europe and the Mediterranean for 12 April 1983 (upper), and 5-day forecasts verifying on this date produced by the then-operational model (middle) and by the new model with envelope orography (lower).

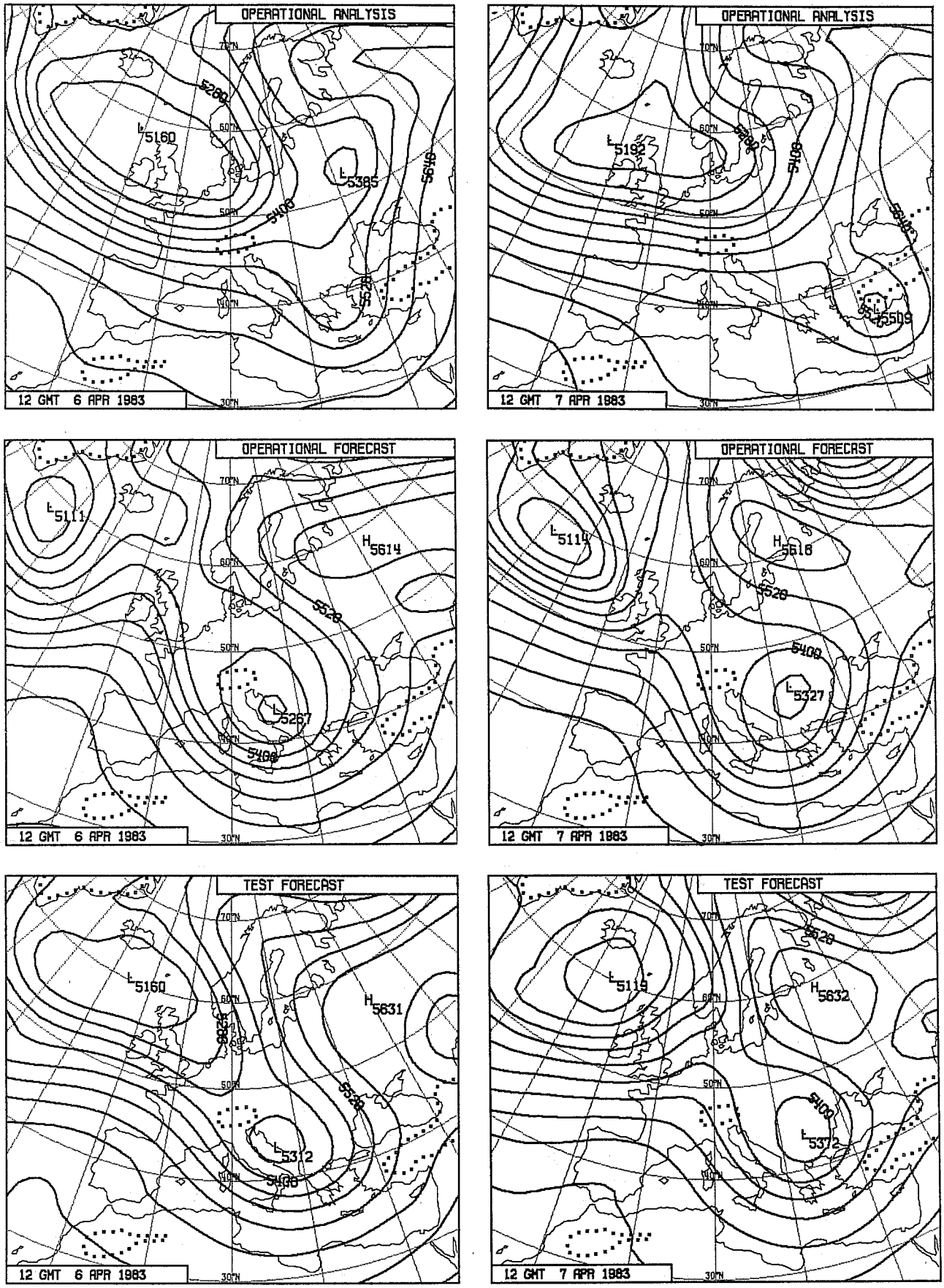

Fig. 17 500 mb height maps as in Fig. 13, but for 6 and 7 April 1983, and day-4 and day-5 forecasts.

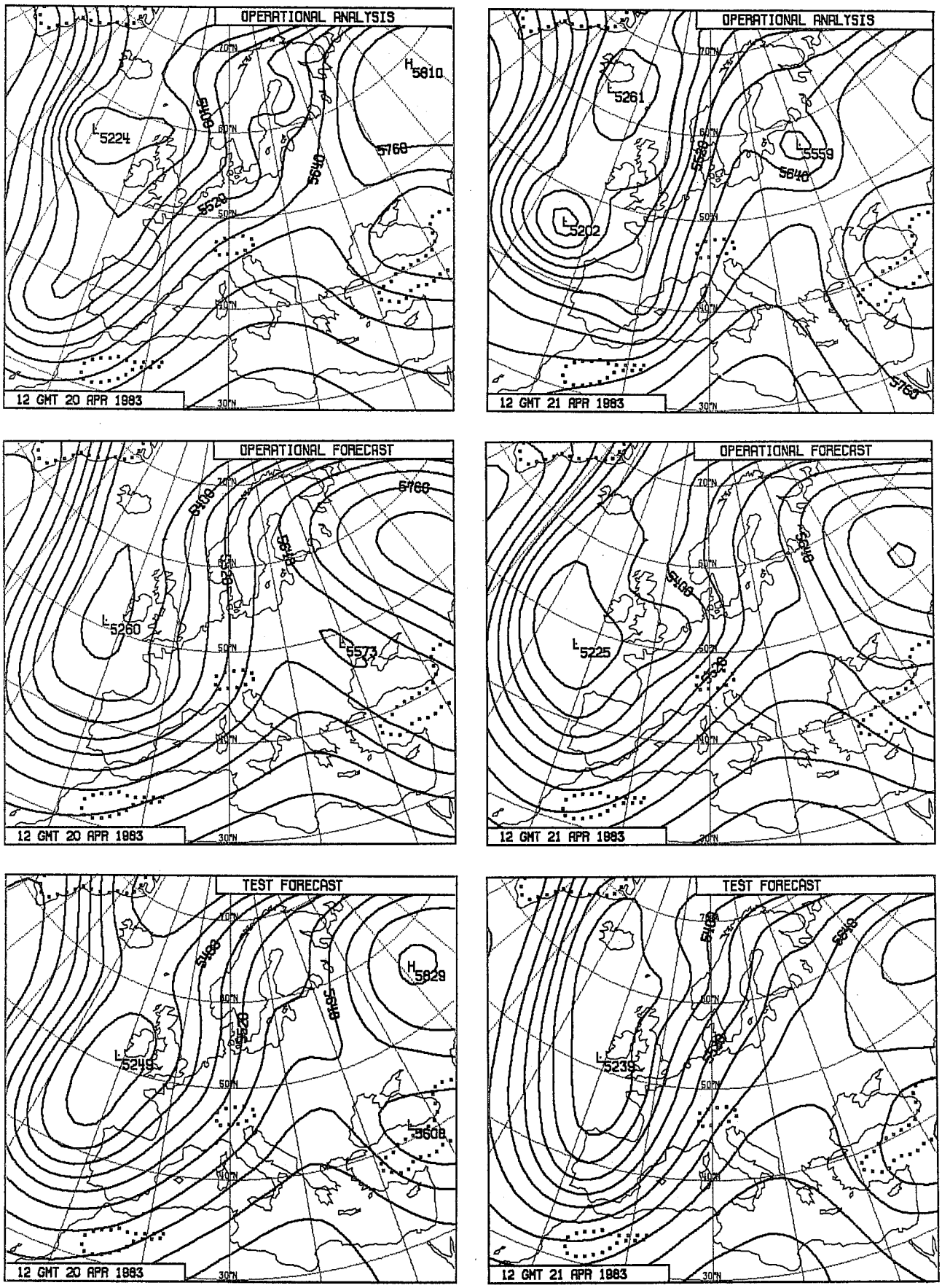

D+5 D+6

Fig. 18 500 mb height maps as in Fig. 13, but for 20 and 21 April 1983.

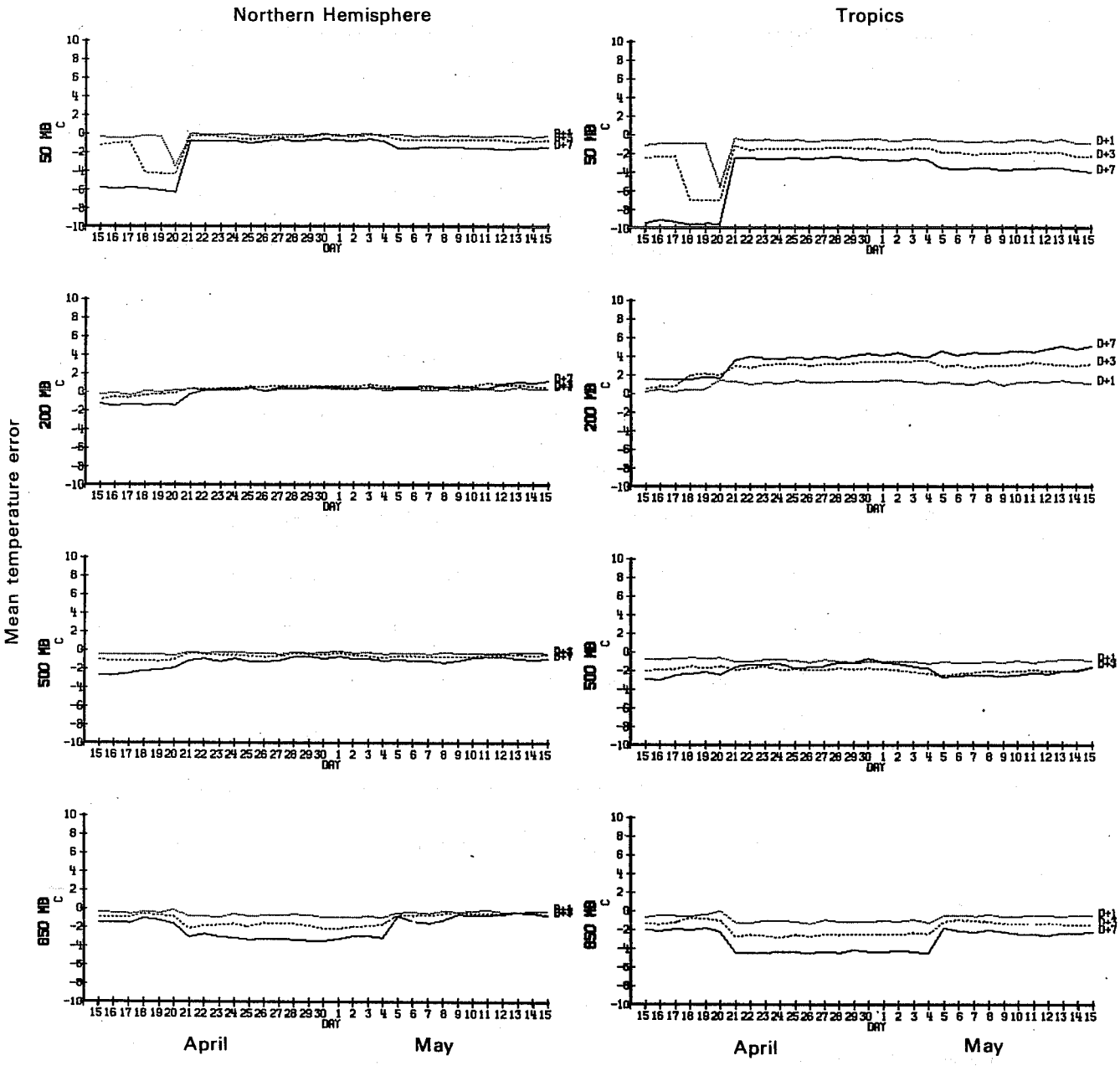

Fig. 19 Mean temperature errors for the Northern Hemisphere (left) and Tropics (right) at the 50, 200, 500 and 850 mb levels. Results are shown for 1-, 3- and 7-day operational forecasts performed from starting dates between 15 April and 15 May 1983.

Results from the winter tests are shown in Figure 11. Here the new-model forecasts actually appear poorer in the short range, although beyond day 5 a rather larger improvement is suggested at 500mb than is indicated by use of anomaly correlations. The parallel-run results in Figure 12 show conversely a distinct improvement of the short-range forecasts, and these results are very clearly in favour of the new system throughout the forecast range.

In the middle of the forecast range, improvements occur in almost every single case when the new forecasting system is used. This can be seen in Fig. 13, which comprises scatter diagrams showing anomaly correlations of 1000 and 500mb height at day 5. Earlier and later in the forecasting period a less decisive result is found, although a clear majority of cases is better up to day 10 with the new system. Fig. 13 also shows that the improvements brought about by the new system, though distinct, are small when compared with the variations in forecast accuracy that occur from case to case. The results of the parallel run are, however, encouraging in that they provide some indication that the largest improvements at 1000mb occur in cases of relatively low overall accuracy.

As an example of a substantial improvement in the quality of the forecast over Europe, we consider the case of 7 April from the parallel run. This was chosen because it displayed the largest difference in hemispheric 1000mb height anomaly correlation in the day-5 results illustrated in Fig. 13. Forecasts of 500mb heights at days 5 and 6 are compared with verifying analyses over Europe in Fig. 14, and corresponding 1000mb maps are shown in Fig. 15. Both forecasts are in error to the north-west of Europe, but the test model clearly gives superior results over the continent itself. At 500mb the sharpness of the major trough is much better represented by the new forecasting system, which also gives an indication of the formation at day 6

of a new centre near the Alps, although the location and intensity of this feature are not accurately captured. At the surface, the overdevelopment of the Eastern European low-pressure region by the then-operational model does not occur in the test forecast, although in the latter there is small-scale overdevelopment south of the Alps and over the Iberian Peninsula at day 5. Despite this, the 5-day forecasts of 850mb wind are substantially better from the new model over much of Southern Europe and the Mediterranean, as can be seen by reference to Fig. 16.

500 mb forecasts for two other cases from the parallel run are compared over Europe in Fig. 17 and 18. The forecasts from 2 April shown for days 4 and 5 in Fig. 17 were unusually poor, and the new model in this case exhibits a negligible improvement in the handling of the trough over the Mediterranean. It is, however, substantially better, though by no means perfect, in its prediction of the flow associated with the low centre to the north-east of the United Kingdom.

Fig. 18 shows 5- and 6-day forecasts from 15 April. At day 5 the test model is more accurate in its treatment of both the trough over the west of the region and the blocking pattern in the east. This extra accuracy is carried over into the 6-day forecast, although by this time neither model has correctly reproduced the small-scale detail shown on the analyzed map.

Only one aspect of the comparison of systematic model errors gave cause for serious concern during the final pre-operational trial. The new model was found to cool substantially more than the old one at low levels, particularly over the tropical and subtropical oceans. Soon after the operational implementation of the model on 21 April this deficiency was traced to an unexpected sensitivity to changes that had been made to the radiation code in

order to include more detailed distributions of aerosols and a representation of the water vapour dimer effect. These changes were removed on 5 May, thus going back to radiative temperature tendencies similar to those of the old operational model pending further research to obtain an improved radiation scheme for future use.

Fig. 19 shows area-mean temperature errors for each 1-, 3- and 7-day operational forecast from 15 April to 15 May. Results are presented separately for the Northern Hemisphere and the Tropics, and the verification is against initialized operational analyses. The increase in 850 mb cooling with the change in operational model on 21 April is evident, as is the reduction in this cooling after 5 May. At other levels there is a general reduction of bias with the introduction of the new system, with the exception of the tropical tropopause where there is an as yet unexplained warming with the new model. The reduction in stratospheric bias is exaggerated in this figure, since a poorer verification of the operational grid-point forecasts is found for the limited number of days when verification was performed using analyses produced by the new system. This should not be taken as indicating entirely a strong model bias to the stratospheric analyses, as bias is also introduced by the vertical interpolation method used to compute a 50 mb temperature from model data for which the nearest available levels are 25 and 75 mb.

Comment on one other systematic error is also appropriate. The development of the experimental programme with the envelope orography was stimulated by noting that mean short-range errors in the predicted height fields showed distinctive negative centres located where mid-latitude jetstreams crossed major mountain ranges. This was interpreted as indicating inadequate orographic forcing in the forecast model. During the parallel run, the

operational grid-point model forecasts using a mean orography repeated this defect, exhibiting largest negative errors in the one-day height forecasts at the two points where the upper-level flow crossed the Rocky Mountain chain. However, only very slightly smaller errors were found with the new model and envelope orography. Reasons for this have yet to be determined, and the performance of the new model in the vicinity of the major mountain ranges is the subject of continuing study.

10. THE OVERALL OPERATIONAL PERFORMANCE

A number of detailed aspects of the behaviour of the new model and orography in operational forecasting have been discussed at relevant points in the preceding text. In attempting to assess more generally the performance of the new system, and in particular to determine the extent to which the improvements indicated by the pre-operational trials have carried over into operational prediction, we encounter two difficulties. The main method open to us is the comparison of results available from the first six months of operational implementation with those from the corresponding six months from 1982. The principal drawback of this approach, particularly as it is applied further into the medium range, is the unknown effect of the substantial variations in predictability that can occur from one month to another. Secondly, a number of other changes to the data assimilation and parameterizations were made between the summer of 1982 and 1983, although these are not thought to have had a substantial impact on extratropical forecast quality.

To avoid as far as possible the efforts of variations in predictability we have compared objective verifications for six-monthly means. To illustrate the results, we present anomaly correlations at 500 and 1000 mb averaged for the months of May to October in Fig. 20 for the extratropical Northern

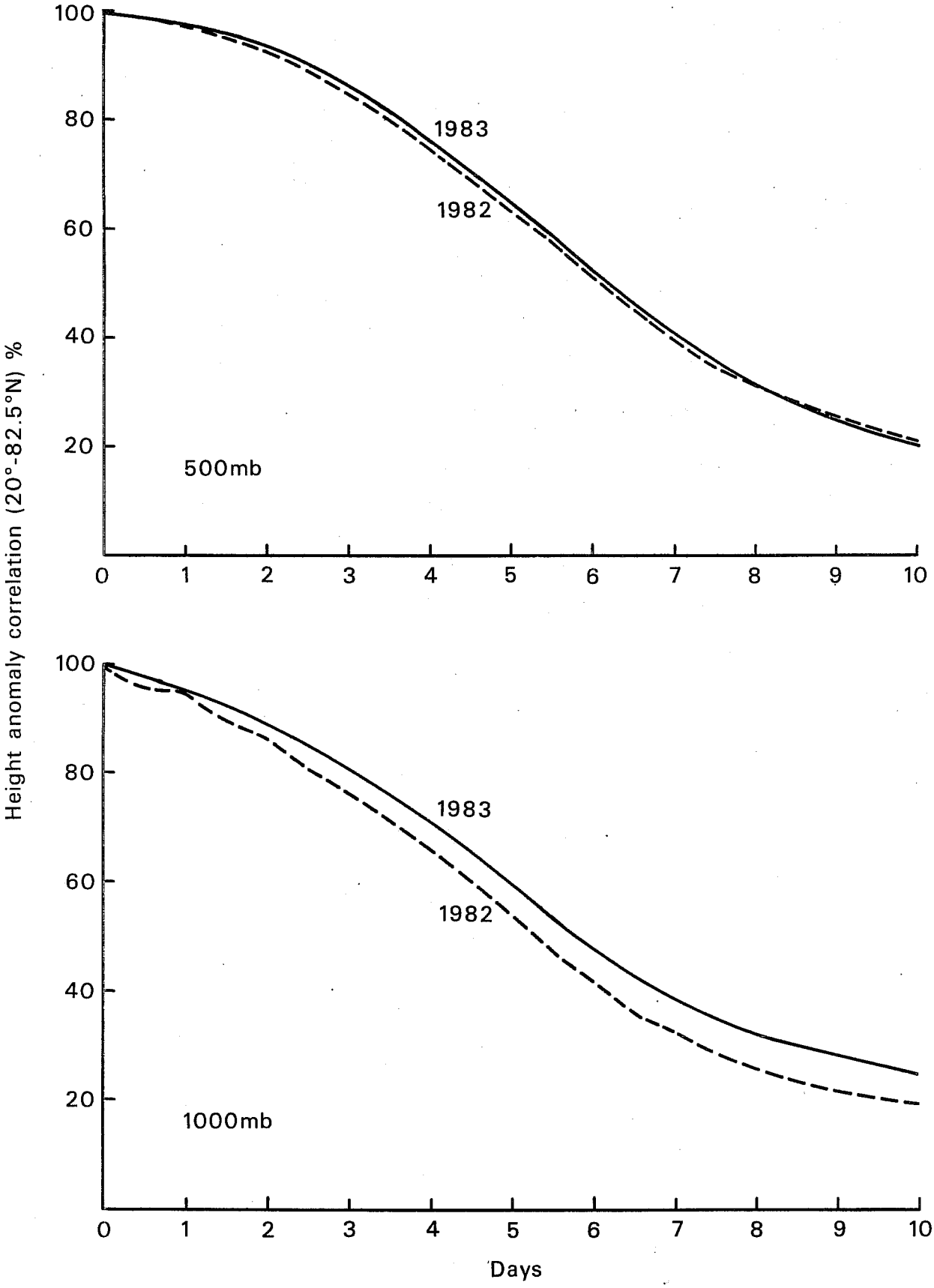

Fig. 20 Mean anomaly correlation of 500mb height (upper) and 1000mb height (lower) for the extratropical Northern Hemisphere, plotted as functions of the forecast range in days. Averages are for the months from May to October inclusive, for 1982 (dashed) and 1983 (solid).

Hemisphere. At 1000 mb there is a clear improvement of the 1983 results over those of 1982, and the increase in predictability of around 12 hours beyond day 2½-3 is largely consistent with the results of the earlier trials. Improvements at 1000 mb in the very short range appear from study of individual monthly verifications to derive largely from the change to a diabatic initialization procedure near the end of September, 1982, and may be to some extent apparent rather than real due to improvements in the (initialized) analyses used for verification.

A much smaller improvement is seen at 500 mb. That at day 2 and 3 occurs systematically from month to month, and is presumably indicative of an improvement of the forecasting system. Beyond day 4, differences in performance between 1982 and 1983 change markedly from one month to the next, and it is difficult to ascribe significance to the small mean 500 mb differences for the latter half of the forecast period. Nevertheless, these results clearly do not show the distinct improvement at 500 mb in the later medium range that has been found to result from use of the envelope orography in winter situations. Consistent with this, tests performed recently for a sample of forecasts for summer 1983, drawn at approximately fortnightly intervals, showed on average somewhat better results using a mean rather than envelope orography, although the apparently detrimental effect of the envelope orography was generally smaller than the beneficial effects seen for winter forecasts. These and additional cases are currently the subject of further study.

11. CONCLUDING REMARKS

In this paper we have outlined some aspects of the design and performance of ECMWF's new operational model. The novel features of this model have generally worked well, both in the pre-operational tests that have been

carried out and during the seven months of operational forecasting that have elapsed at the time of writing. The flexibility and general construction of the code of the new model should facilitate its future use for a wide range of research.

Final trials and the results from six months of operational prediction indicate that the new spectral, hybrid-coordinate model with envelope orography performs distinctly better than the grid-point sigma-coordinate model with mean orography previously used in operational forecasting. Objective verification suggests that this amounts to an average increase in medium-range predictability which can lie in the range from 12 to 24 hours depending on the atmospheric level, the range of the forecast, the season, and the measure of skill that is adopted. Improvements are found in general throughout the 10-day forecast range. Subjective synoptic assessment confirms the results of the objective verification.

When judged in the context of the overall development of numerical weather prediction, improvements of the degree indicated here undoubtedly represent a significant step forward, but our results must be treated with some caution. Interannual variations in predictability are sufficiently large to cast some doubt on the generality of the results presented here. For example, in the comparison of spectral and grid-point models by Girard and Jarraud (1982), the forecasts for the winter of 1979/80 showed no advantage to the spectral model, and studies of the impact of the envelope orography have shown a marked variability with synoptic situation. Nevertheless, it is perhaps worth recalling here that quite a wide range of accuracy was encountered in the sets of pre-operational trial forecasts, and the new system appeared to give better results across the whole of this range.

A number of specific deficiencies in performance or uncertainties in formulation have been noted in preceding sections. Some attention has been devoted to these and will continue, but further efforts at the fine tuning of, for example, the orography or diffusion will be limited. Instead, emphasis will increasingly be placed on development of an effective higher resolution version, with improved parameterization schemes, for use on the CRAY X-MP recently acquired by ECMWF.

ACKNOWLEDGEMENTS

Particular mention should be made of the contributions of C. Girard and J-F. Geleyn to the scientific design of the model, of J.M. Wallace and S. Tibaldi to the study of orographic representation, and of R. Gibson, J. Haseler and J-F. Geleyn to the design and production of the computer code of the model, post-processing and analysis interface. Contributions from J. van Maanen and W. Wergen in the areas of analysis and initialization are also acknowledged, as are the efforts of many members of the Operations Department to ensure a timely and relatively trouble-free execution and analysis of the parallel run and operational implementation. We are also grateful to the many other members of the Research Department who assisted with this work in various ways.

References

Asselin, R. 1972: Frequency filter for time integrations. Mon.Wea.Rev., 100, 487-490.

Baede, A.P.M., Jarraud, M. and Cubasch, U., 1979: Adiabatic formulation and organisation of ECMWF's spectral model. ECMWF Tech.Rep.No.15, 40 pp.

Bourke, W. 1974: A multi-level spectral model: I Formulation and hemispheric integrations. Mon.Wea.Rev., 102, 688-701.

Cline, A.K. 1974: Scalar- and planar-valued curve fitting using splines under tension. Communications of the ACM, 17, 218-220.

Dell'Osso, L. 1983: High resolution experiments with the ECMWF model: A case study. ECMWF Technical Report No. 37. 53 pp.

Gibson, J.K. 1983: A simple memory manager. ECMWF Tech.Memo.No.73, 9 pp.

Girard, C., and Jarraud, M., 1982: Short and medium range forecast differences between a spectral and grid point model. An extensive quasi-operational comparison. ECMWF Tech.Rep.No.32, 178 pp.

Hoskins, B.J. and Simmons, A.J. 1975: A multi-layer spectral model and the semi-implicit method. Quart.J.R.Met.Soc., 101, 637-655.

McIntyre, M.E. and T.N. Palmer 1983: Breaking planetary waves in the stratosphere. Nature, 305, 593-600.

Robert, A.J. 1981: A stable numerical integration scheme for the primitive meteorological equations. Atmos.Ocean, 19, 35-46.

Simmons, A.J. 1983: Adiabatic formulations of the ECMWF forecasting system. Proceedings of 1982 ECMWF Seminar/Workshop on Interpretation of Numerical Weather Prediction Products, 59-72.

Simmons, A.J. and Strüfing, R. 1981: An energy and angular-momentum conserving finite-difference scheme, hybrid coordinates and medium-range weather prediction. ECMWF Tech.Rep.No.28, 68 pp.

Wallace, J.M., Tibaldi, S. and Simmons, A.J. 1983: Reduction of systematic forecast errors in the ECMWF model through the introduction of an envelope orography. Proceedings of the ECMWF Workshop on Intercomparion of Large-Scale Models used for Extended Range Forecasting, 371-434.